NAVAL POSTGRADUATE SCHOOL
Monterey, California

THESIS

CALIBRATION TO DETERMINE PRESSURE AND TEMPERATURE SENSITIVITIES OF A PRESSURE-SENSITIVE PAINT

by

Judith A. Muller

June 2000

Thesis Advisor: Raymond P. Shreeve

Approved for public release; distribution is unlimited.

REPORT DOCUMENTATION PAGE		Form Approved OMB No. 0704-0188

Public reporting burden for this collection of information is estimated to average 1 hour per response, including the time for reviewing instruction, searching existing data sources, gathering and maintaining the data needed, and completing and reviewing the collection of information. Send comments regarding this burden estimate or any other aspect of this collection of information, including suggestions for reducing this burden, to Washington headquarters Services, Directorate for Information Operations and Reports, 1215 Jefferson Davis Highway, Suite 1204, Arlington, VA 22202-4302, and to the Office of Management and Budget, Paperwork Reduction Project (0704-0188) Washington DC 20503.

1. AGENCY USE ONLY *(Leave blank)*	2. REPORT DATE June 2000	3. REPORT TYPE AND DATES COVERED Master's Thesis
4. TITLE AND SUBTITLE: CALIBRATION TO DETERMINE PRESSURE AND TEMPERATURE SENSITIVITIES OF A PRESSURE-SENSITIVE PAINT		5. FUNDING NUMBERS
6. AUTHOR(S) Muller, Judith A.		
7. PERFORMING ORGANIZATION NAME(S) AND ADDRESS(ES) Naval Postgraduate School Monterey, CA 93943-5000		8. PERFORMING ORGANIZATION REPORT NUMBER
9. SPONSORING / MONITORING AGENCY NAME(S) AND ADDRESS(ES) N/A		10. SPONSORING / MONITORING AGENCY REPORT NUMBER
11. SUPPLEMENTARY NOTES The views expressed in this thesis are those of the author and do not reflect the official policy or position of the Department of Defense or the U.S. Government.		
12a. DISTRIBUTION / AVAILABILITY STATEMENT Approved for public release; distribution is unlimited.		12b. DISTRIBUTION CODE

ABSTRACT *(maximum 200 words)*

In order to obtain quantitative surface pressure measurements of a transonic compressor rotor using pressure sensitive paint (PSP), the temperature dependence of the paint must be taken into consideration. In the present study, a calibration chamber was built and instrumented such that pressure and temperature could be controlled independently. Photodiodes were used to measure the intensity of light emitted by the PSP. An acquisition program was developed to record the necessary calibration data to obtain an analytical representation of the luminescent response of the pressure-sensitive paint over a range of pressures and temperatures characteristic of transonic fans.

14. SUBJECT TERMS Pressure-Sensitive Paint, Photoluminescence, Luminescence, PtOEP, UV Illumination, Detection, Emission, Aerodynamics, Measurements, Temperature and Pressure Calibration			15. NUMBER OF PAGES 96 16. PRICE CODE
17. SECURITY CLASSIFICATION OF REPORT Unclassified	18. SECURITY CLASSIFICATION OF THIS PAGE Unclassified	19. SECURITY CLASSIFICATION OF ABSTRACT Unclassified	20. LIMITATION OF ABSTRACT UL

NSN 7540-01-280-5500

Standard Form 298 (Rev. 2-89)
Prescribed by ANSI Std. 239-18

THIS PAGE INTENTIONALLY LEFT BLANK

Approved for public release; distribution is unlimited.

CALIBRATION TO DETERMINE PRESSURE AND TEMPERATURE SENSITIVITIES OF A PRESSURE-SENSITIVE PAINT

Judith A. Muller
Ensign, United States Navy
B.S., Rensselaer Polytechnic Institute, 1999

Submitted in partial fulfillment of the
requirements for the degree of

MASTER OF SCIENCE IN AERONAUTICAL ENGINEERING

from the

NAVAL POSTGRADUATE SCHOOL
June 2000

Author: 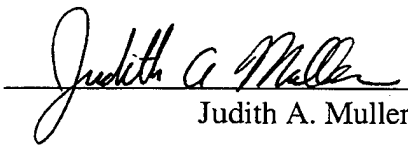
Judith A. Muller

Approved by: 
Raymond P. Shreeve, Thesis Advisor

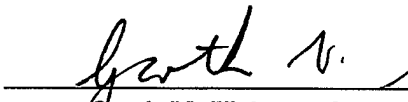
Garth V. Hobson, Second Reader


Max F. Platzer, Chairman
Department of Aeronautics and Astronautics

THIS PAGE INTENTIONALLY LEFT BLANK

ABSTRACT

In order to obtain quantitative surface pressure measurements of a transonic compressor rotor using pressure sensitive paint (PSP), the temperature dependence of the paint must be taken into consideration. In the present study, a calibration chamber was built and instrumented such that pressure and temperature could be controlled independently. Photodiodes were used to measure the intensity of light emitted by the PSP. An acquisition program was developed to record the necessary calibration data to obtain an analytical representation of the luminescent response of the pressure-sensitive paint over a range of pressures and temperatures characteristic of transonic fans.

THIS PAGE INTENTIONALLY LEFT BLANK

TABLE OF CONTENTS

THIS PAGE INTENTIONALLY LEFT BLANK

LIST OF FIGURES

LIST OF TABLES

THIS PAGE INTENTIONALLY LEFT BLANK

ACKNOWLEDGEMENTS

I would like to extend my appreciation to everyone at the Turbo-Propulsion Lab for all of the support that they gave me.

I would like to thank Professor Raymond Shreeve, for providing the opportunity to complete this research. His calm guidance through the experimentation and writing processes made it possible.

I would also like to thank Doug Seivwright for endlessly attaching thermocouples and answering questions. His extensive knowledge of the subject made it possible to complete the present work in the time required.

And finally, I would like to thank Rick Still and John Gibson for helping me put everything together and keeping me smiling when things went wrong.

Special thanks to everyone for making the Turbopropulsion Lab a wonderful place to work, learn, and form friendships.

I. INTRODUCTION

The motivation for the present research was the use of pressure-sensitive paint (PSP) to obtain the pressure distribution on a transonic rotor. The first intended application was the rotor tested by Grossman in [Ref. 1]. PSP would provide a complete surface pressure mapping that could be compared to computational fluid dynamics (CFD) results. The results would serve to verify CFD analysis code predictions and the use of CFD as a design tool.

Varner [Ref. 2] and Quinn [Ref. 3] developed procedures for acquiring low intensity luminescence from a high-speed rotor using nano-second shutter speeds, phase-locked imaging, and a charge-coupled-device (CCD) camera. These methods demonstrated the potential of surface pressure mapping; however, temperature sensitivities of the paint prevented quantitative measurements.

In order to obtain quantitative results, pressure and temperature sensitivities of the paint must be taken into consideration [Ref. 4]. To accomplish this, an analytical representation of the pressure and temperature dependent characteristics of the paint must be derived [See Appendix A]. Accurate, detailed calibration data must be obtained, to determine the temperature dependent coefficients of the paint.

The purpose of the present study was to develop a bench-top apparatus, controls, and data acquisition system to accurately calibrate the luminescent response of the pressure-sensitive paint, over a range of pressures and temperatures characteristic of transonic fans. For the present study, the pressure-sensitive paint used was Platinum

octaethylporphyrin (PtOEP). The calibration apparatus was built and instrumented. A program was written to control the apparatus and record the necessary data. Several sets of data were taken and a preliminary calibration representation was derived from the results.

II. BACKGROUND

A. PHOTOCHEMISTRY

The properties of PtOEP that allow it to be used for PSP measurements can be explained by basic principles of quantum mechanics and photochemistry. According to quantum theory, molecules have discrete, quantized energy levels. Molecules usually exist at the lowest energy level, called the ground state. The energy of the molecule can be raised, placing it in an excited state. Excited states only exist in defined levels, each requiring a specific amount of energy to achieve the excited state. When the proper amount of energy is added to a molecule, an excited state can be achieved. This energy can be in the form of a photon; the energy of a photon is given by $E = h\nu$, where h is Planck's constant, 6.6256×10^{-34} J s, and ν is the frequency of the photon. Each energy level has a range of vibrational energies which electrons can have. These vibrational energies can cause the energy levels to have some overlap.

Luminescence is a process by which a molecule can go from an excited state back to its ground state, by emitting a photon. Luminescence includes two subcategories, fluorescence and phosphorescence. The difference between fluorescence and phosphorescence is the amount of time between the end of the excitation of the molecule and the emission of the photon. For fluorescence, the process takes between 10^{-9} and 10^{-7} seconds, whereas phosphorescence takes between 10^{-4} and 10^{-2} seconds. Photoluminescence is defined as light emission excited by light absorption.

Any given molecule can have several energy levels for a single configuration of the molecule, based on different combinations of electron spin direction and orbit. This is called Russell Sanders coupling [Ref. 5]. Electrons are usually found in pairs, where the electrons are spinning in opposite directions. The opposing spins of the electron pair effectively cancels out any effect that they might have, resulting in a single energy level called a singlet state. It is also possible for a pair of electrons, in an excited state, to have the same spin direction, resulting in three possible energy level configurations, or a triplet state. Every excited singlet state has a corresponding triplet state, which has a lower energy level. According to the spin multiplicity rule, electromagnetic radiation does not change the spin direction of electrons; therefore, a photon can only excite a molecule from a singlet state to a singlet state.

There are several ways for an excited molecule to move to a lower energy state. The first method is by fluorescence. A second method is called internal conversion. Internal conversion occurs when the electron crosses from a low vibrational energy at a higher level, to a higher vibrational energy at a lower level; both electrons have the same amount of total energy. The excess vibrational energy of the excited molecule is then dissipated by collisions with other molecules, allowing it to return to a low vibrational energy level at the ground state. The third method is called intersystem crossing. Intersystem crossing is similar to internal conversion in that the electron moves laterally from low vibrational energy at a higher state to higher vibrational energy at a lower state; but the electron must also change its spin direction to move from a singlet to a triplet state. Spin orbit reversal can occur under two circumstances. The first, spin-orbit

coupling, occurs in heavy atoms, such as PtOEP, when the rotation of the electron around the nucleus generates a magnetic force strong enough to reverse the spin direction. The second is when unpaired electrons, such as those found in oxygen molecules, tend to breakdown the spin selection rules [Ref. 6].

If the molecule moves from the excited singlet state into the excited triplet state, there are two ways for it to continue to a ground state. The first is by intersystem crossing and the second is by phosphorescence. In either case, the excited molecule returns to its ground state. The following is a list of possible reactions for an excited molecule to return to its ground state, and the approximate frequency of occurrence. Figure 1 shows a visual representation of these reactions.

$S_1 \rightarrow S_0$; Internal conversion, $10^6 - 10^{12}\ s^{-1}$ (Vibrational Quenching, $10^{12}\ s^{-1}$)

$S_1 \rightarrow S_0 + h\nu$; Fluorescence, $10^6 - 10^9\ s^{-1}$

$S_1 \rightarrow T_1$; Intersystem crossing, $10^4 - 10^{12}\ s^{-1}$ (Vibrational Quenching, $10^{12}\ s^{-1}$)

$T_1 \rightarrow S_0$; Intersystem crossing, $10^{-1} - 10^5\ s^{-1}$ (Vibrational Quenching, $10^{12}\ s^{-1}$)

$T_1 \rightarrow S_0 + h\nu$; Phosphorescence, $10^{-2} - 10^4\ s^{-1}$

Since internal conversion, fluorescence, and intersystem crossing from S_1 to T_1 all take approximately the same amount of time, there is a good opportunity for each to occur. If the internal conversion process was more efficient, as it is when the energy levels are closer together, there would not be a chance for the fluorescence and intersystem crossing to take place, and the paint would not be effective. Similarly, if the intersystem crossing was as inefficient as it is between T_1 and S_0, it would not be able to compete with the fluorescence, and there would be little phosphorescence. Also, if the

intersystem crossing between T_1 and S_0 was more efficient, it would dominate the phosphorescence, again preventing the desired luminescent response.

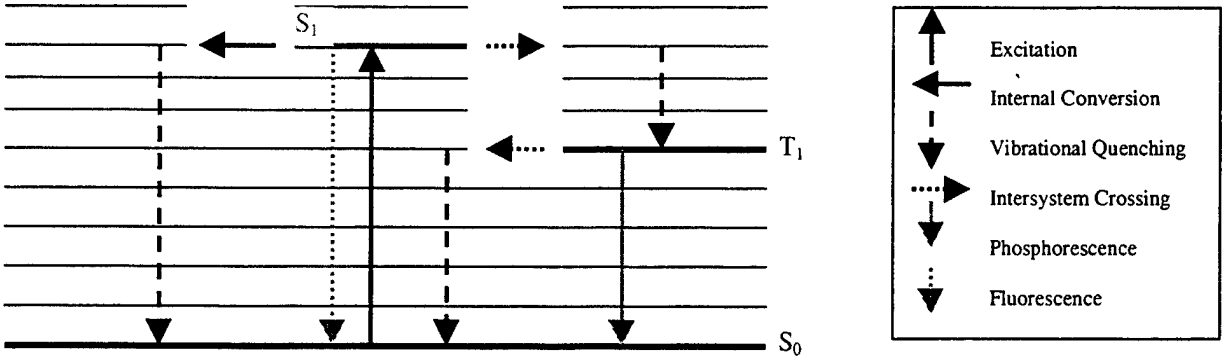

Figure 1. Summary of Possible Molecular Reactions.

PtOEP has two absorption peaks, one in the ultraviolet range, at 380 nm, and a smaller one at 540 nm, in the green region. The emission from PtOEP is in the red region, at approximately 650 nm. These ranges can be seen in Figure 2.

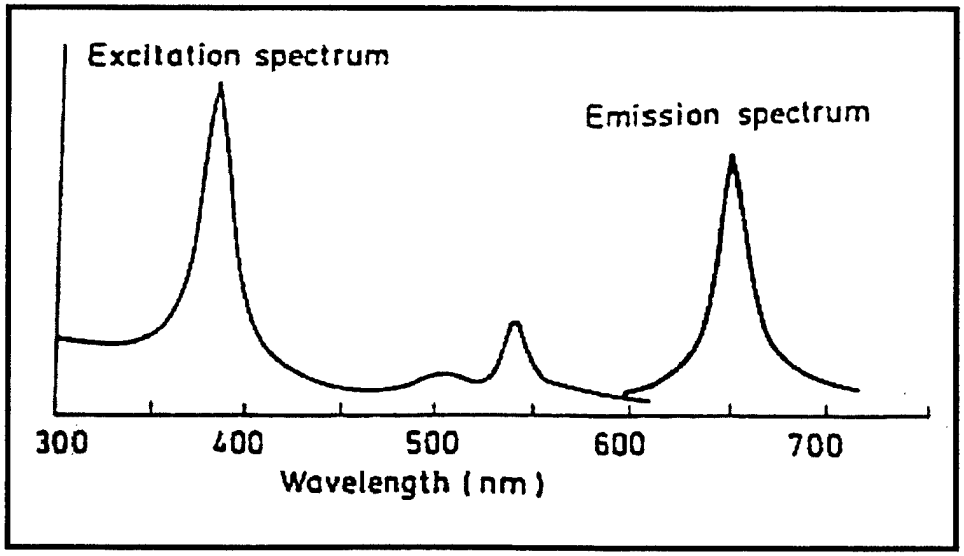

Figure 2. Excitation and Emission Spectrum of PtOEP.

B. OXYGEN QUENCHING

The ground state of the oxygen molecule is a triplet state since it has two unpaired electrons in different orbitals. As mentioned earlier, this can lead to the breakdown of spin selection rules. Oxygen has the capability to easily remove excitation energy from other molecules, as shown in the following reaction:

$$T_1 + {}^3O_2 \rightarrow S_0 + {}^1O_2$$

Where T_1 is the first triplet state and S_0 is the ground singlet state.

When PtOEP is excited in the presence of oxygen, the oxygen interferes with the emission process by causing more intersystem crossing, which causes less phosphorescence than would occur if there were no oxygen molecules present. This process is called oxygen quenching. The higher the concentration of oxygen (i.e., the higher the pressure), the less phosphorescence is observed. The intensity of the phosphorescence can be measured, making it possible to use PtOEP for pressure measurements.

The Stern-Volmer equation is used to describe bimolecular quenching of luminescence.

$$\frac{I_0}{I} = A + B\frac{P}{P_0} \tag{1}$$

This linear approximation can easily be extended to a quadratic form, which better describes experimentally observed behavior [Ref. 3]:

$$\frac{I_0}{I} = A + B\frac{P}{P_0} + C\left[\frac{P}{P_0}\right]^2 \tag{2}$$

C. TEMPERATURE SENSITIVITY

Unfortunately, PSP is not only sensitive to pressure, but also to temperature. Higher temperatures lead to a longer life of the triplet state. This makes the PtOEP much more susceptible to oxygen quenching. It allows more intersystem crossing to take place, which results in less phosphorescence. The higher the temperature, the less responsive the PSP is to changes in pressure. Typical temperature sensitivities are shown in Figures 3 and 4.

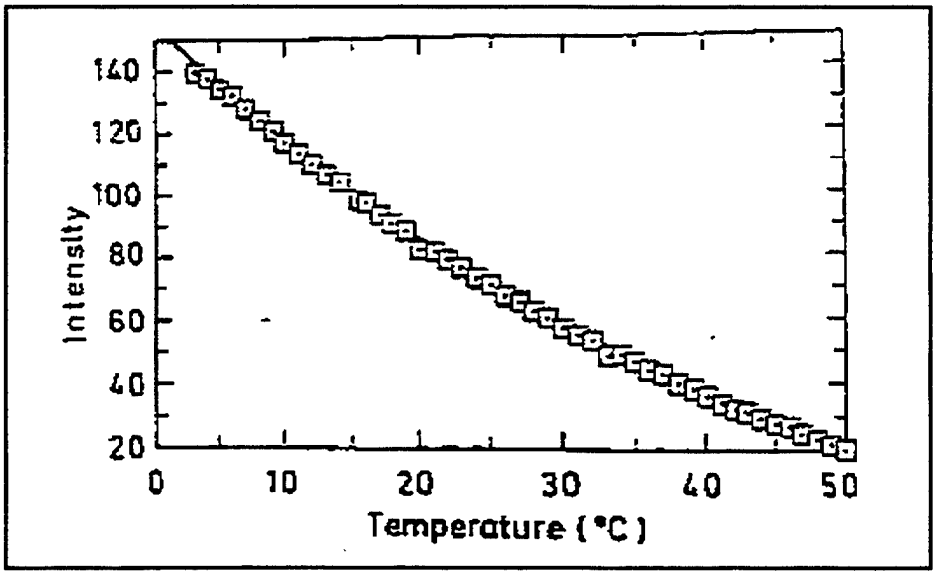

Figure 3. Effect of Temperature on PtOEP Response, [from Ref. 6].

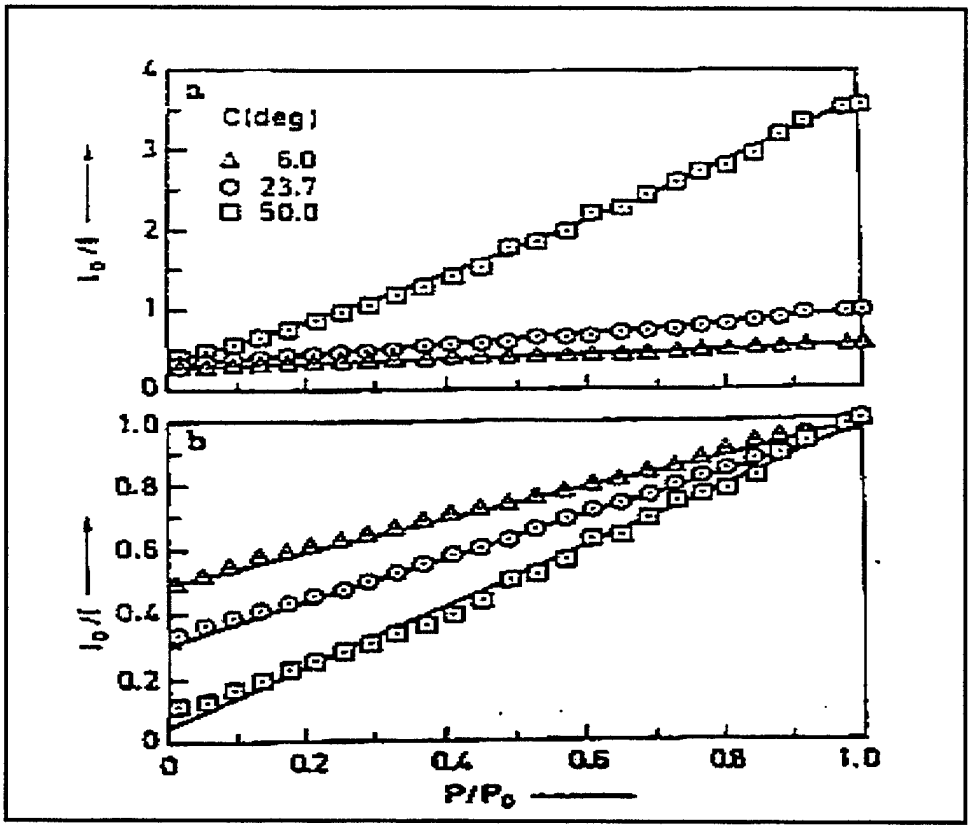

Figure 4. Calibration Curves from Kavandi, [Ref. 6].

(Note: In the top plot of Figure 4, Io was measured at 23.7°C for each curve. In the second plot, Io for each curve was taken at its respective temperature.)

In compressor applications, it is not feasible to keep the surface temperature constant. It is also not possible to accurately measure the temperature at every point on the compressor blade. This makes it necessary to calibrate the PSP, and to devise a technique to derive both temperature and pressure from maps of luminescent intensities. In the present study the first of these goals, to provide a means to calibrate the PSP, and then represent the temperature and pressure dependence analytically, was achieved.

THIS PAGE INTENTIONALLY LEFT BLANK

III. CALIBRATION APPARATUS AND INSTRUMENTATION

A. OVERVIEW

The calibration apparatus was a bench-top setup located in the Gas Dynamics Laboratory (Building 216) at the Naval Postgraduate School. The apparatus is shown in Figure 5, and a schematic of the system is shown in Figure 6.

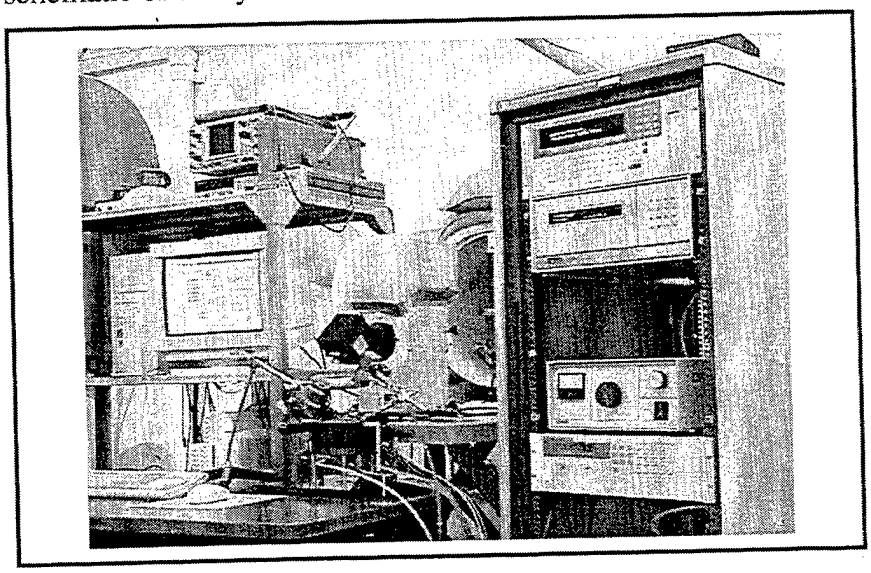

Figure 5. Calibration Setup.

A small (1.25 x 1.50 x .125 inches) aluminum coupon was coated with PSP, and placed in a small windowed chamber, in which pressures varying from 1 psi to 28 psi could be set. The temperature of the sample in the chamber was controlled from approximately 25° F below the temperature of the heat sink to 150° F above the temperature of the heat sink, using a thermoelectric cooler (TEC). These ranges were more than adequate to cover the range of conditions found in single-stage transonic compressor rotor tests, which is approximately .5 to 1.5 atm in surface pressure and 50° F

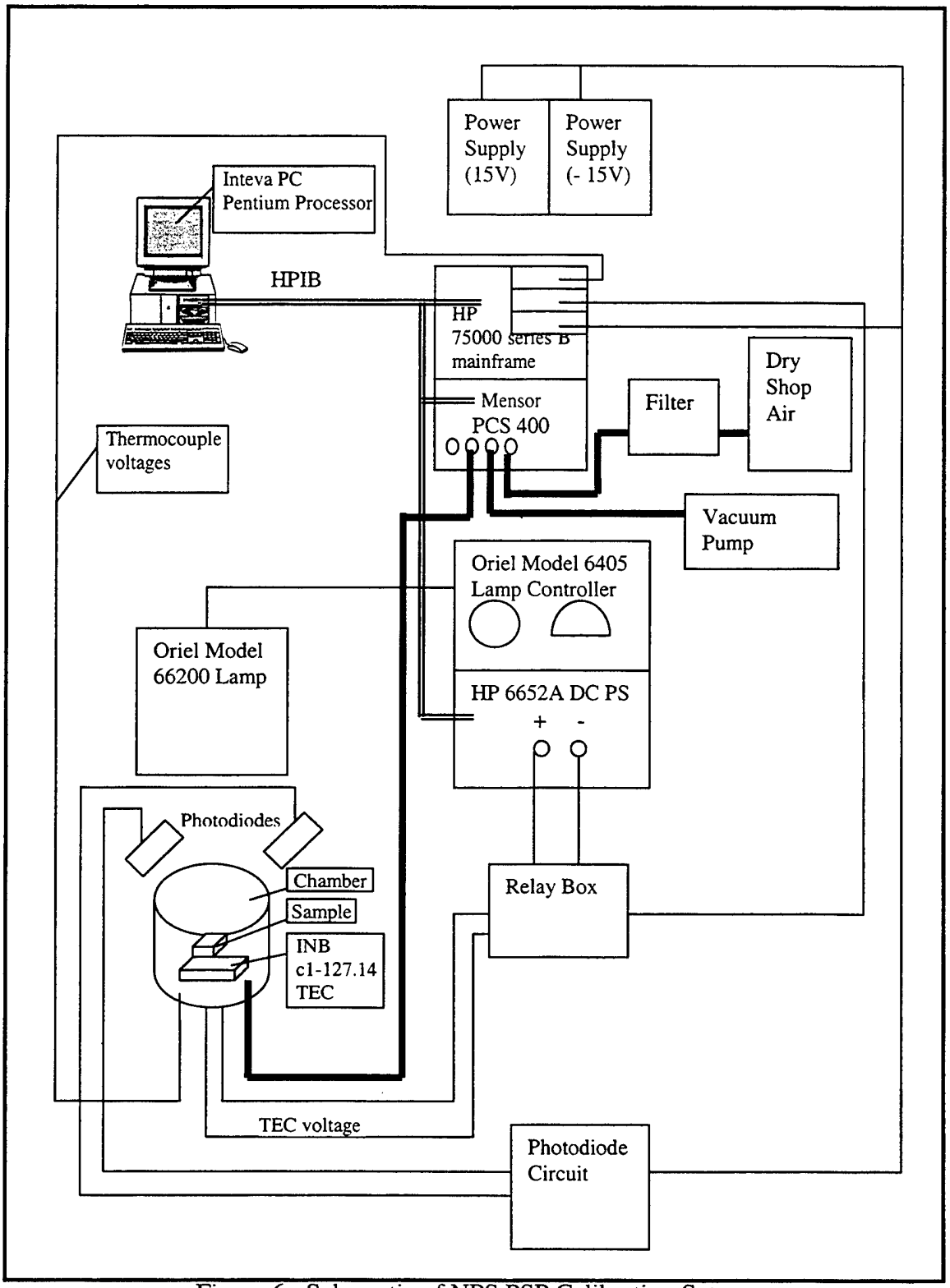

Figure 6. Schematic of NPS PSP Calibration Setup.

to 170° F in surface temperature. A data acquisition and control program was written using Hewlett Packard (HP) Visual Engineering Environment (HP VEE) software. The program allowed the user to set a desired range of values for pressure and temperature. The pressure in the chamber and the temperature of the sample were set by the program, and the values of the pressure, temperature, and intensity from the sample and from the UV lamp were recorded.

B. VACUUM AND PRESSURE CHAMBER

The vacuum and pressure chamber, shown in Figure 7, was based on the design used by Dr. James Bell at NASA-Ames, [Ref. 7]; an assembly drawing is shown in Figure 8. The base was machined from aluminum, and then black anodized with a Teflon coating. The chamber inside diameter was five inches. The base had four ½ inch fittings: one carried two sets of thermocouple wires, one was the pneumatic line, and two carried the power wires to the TEC.

The top of the chamber was brass, which was also blackened. The top was threaded onto the base to provide easy access to the chamber, while providing the necessary structure to sustain both pressure and vacuum. The window was of Plexiglas UVT, which is transparent to the frequencies of the excitation and luminescence of the PSP. The chamber was attached to a heavy steel plate (12 x 12 x 1 inch) using four, four-inch long, 3/8 inch diameter threaded rods, which allowed access to the four fittings in the base.

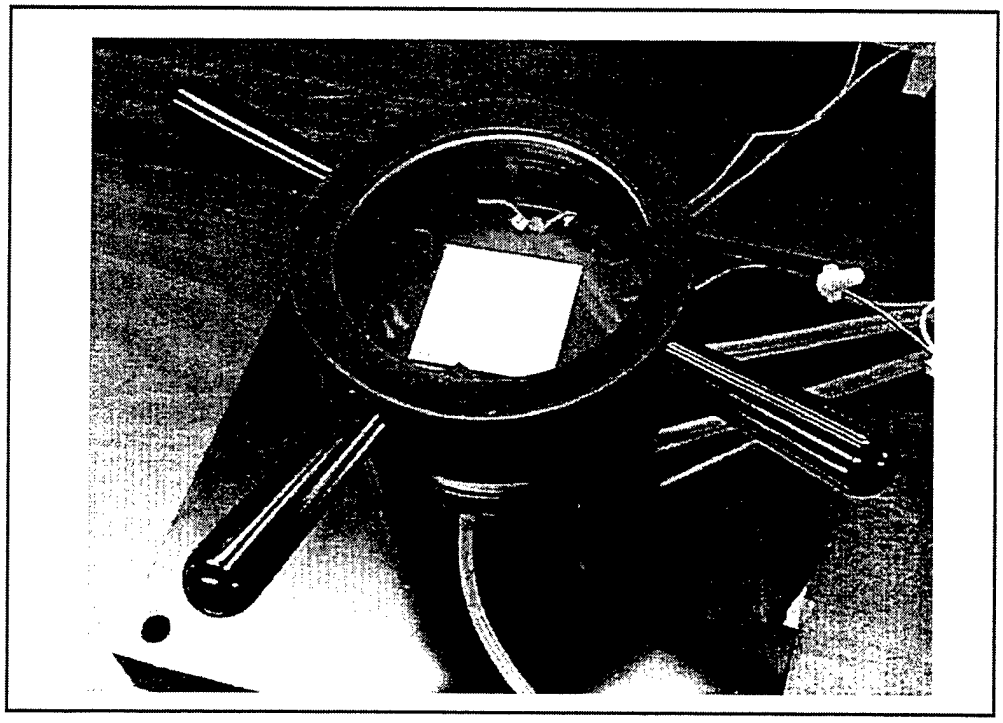

Figure 7. Vacuum and Pressure Chamber.

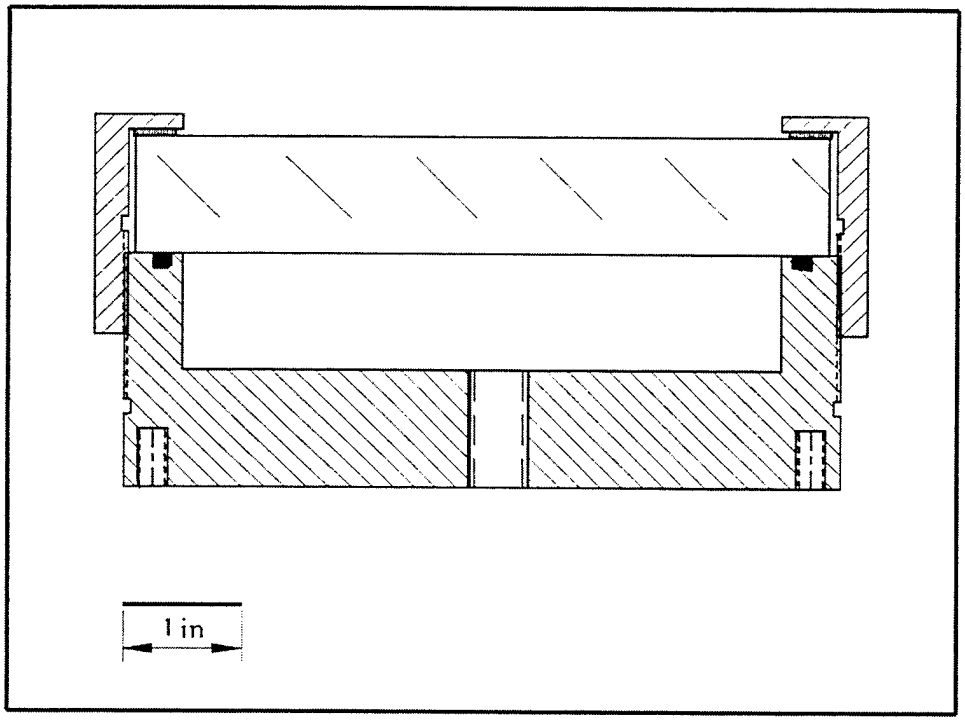

Figure 8. Chamber Assembly Drawing.

C. TEMPERATURE CONTROL

The sample was heated and cooled using an INB Products thermoelectric cooler (TEC), model inbC1-127.14, shown in Figure 9. The voltage applied to the TEC, created a temperature difference between the upper and lower surface. When the voltage was applied in one direction, the upper surface of the TEC was hotter and the lower surface was cooler. If the voltage was reversed, the upper surface was cooler and the lower surface hotter. The sample, painted with PSP, was sealed to the TEC with a thin layer of GC Electronics 10-8135 high thermal conductive heat sink compound. Water was circulated from a faucet, through a cooling coil attached to the underside of the base, and into a drain. The water served to maintain a nearly constant base temperature, so that the direction of the applied voltage either heated or cooled the sample with respect to the water temperature.

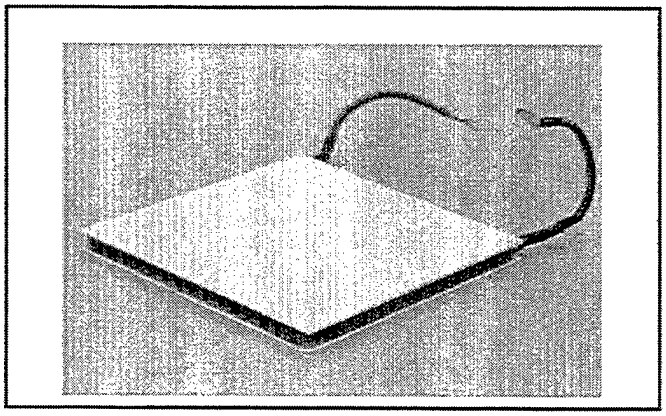

Figure 9. Thermoelectric Cooler (TEC).

A thermocouple was attached to the sample and a thermocouple was attached to the base of the chamber. The thermocouple on the sample was secured with Omegabond

"400" high temperature air set cement, which is resistant to solvents. This was necessary since the PSP binder contained a solvent that would otherwise loosen the thermocouple. The two (type J) thermocouples were connected to channels 1 and 2 of an HP E1347A 16-Channel Thermocouple Relay Multiplexer (MUX), shown in Figure 10. The HP VEE control program acquired the temperatures of the sample and the base at every data point.

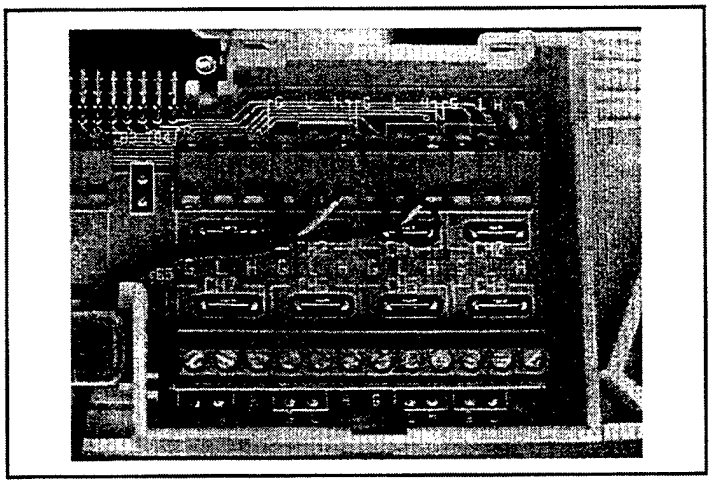

Figure 10. Connections to the 16-Channel Thermocouple Relay Multiplexer.

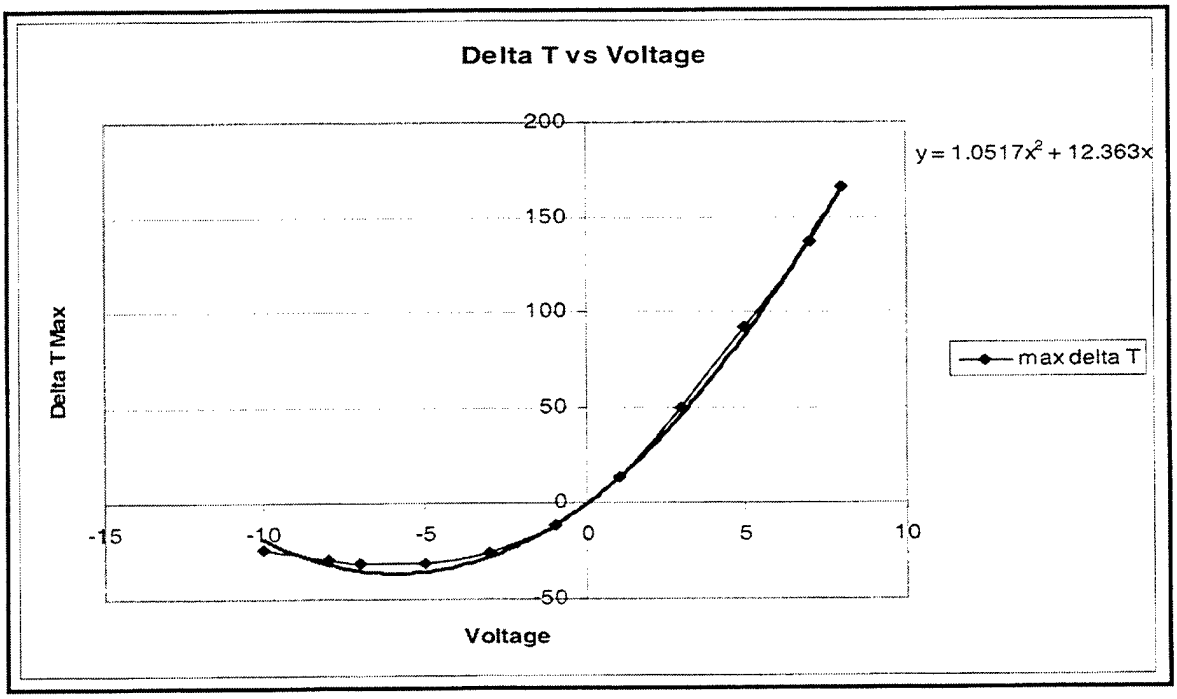

Figure 11. Temperature Response of the TEC.

An HP 6652A DC Power Supply provided the voltage to control the temperature of the TEC. A test was conducted to calibrate the TEC, and the result is shown in Figure 11. The HP VEE control program used the equation of the curve fit to the data shown in Figure 11 to determine the correct voltage to set for a desired sample temperature. The absolute value of the voltage was used, and the direction of the voltage was controlled to effect heating or cooling. The direction of the voltage was controlled using an HP E1364A 16 Channel Form C Switch Module (Figures 12 and 13) and a relay box (Figures 14 and 15), which was made in house. When the sample was to be heated, switches 6 and 7 on the Form C Switch were closed. This closed relays 1 and 2, which allowed the voltage set on the HP 6652A Power Supply to feed the TEC in the heating direction. To cool the sample, switches 8 and 9 were closed, closing relays 3 and 4, and allowing the voltage to feed the TEC in the opposite direction.

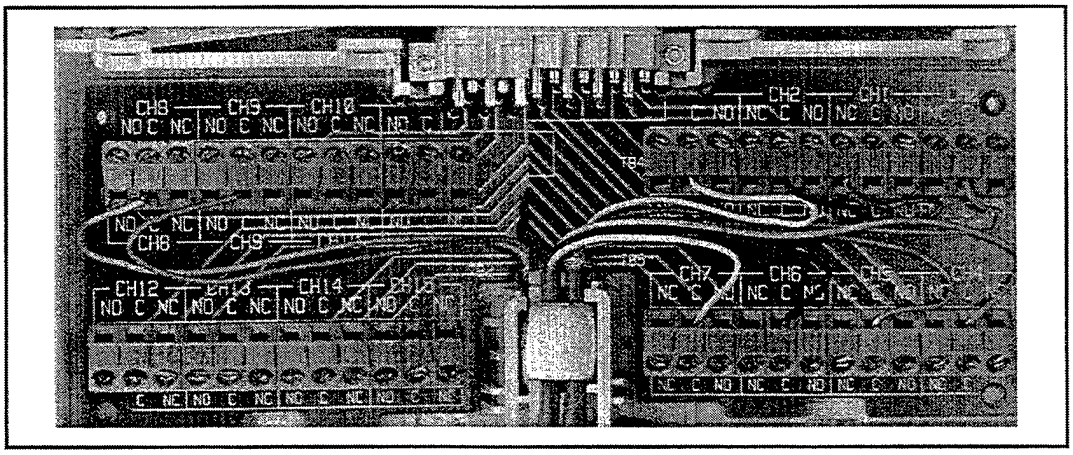

Figure 12. Form C Switch Connections.

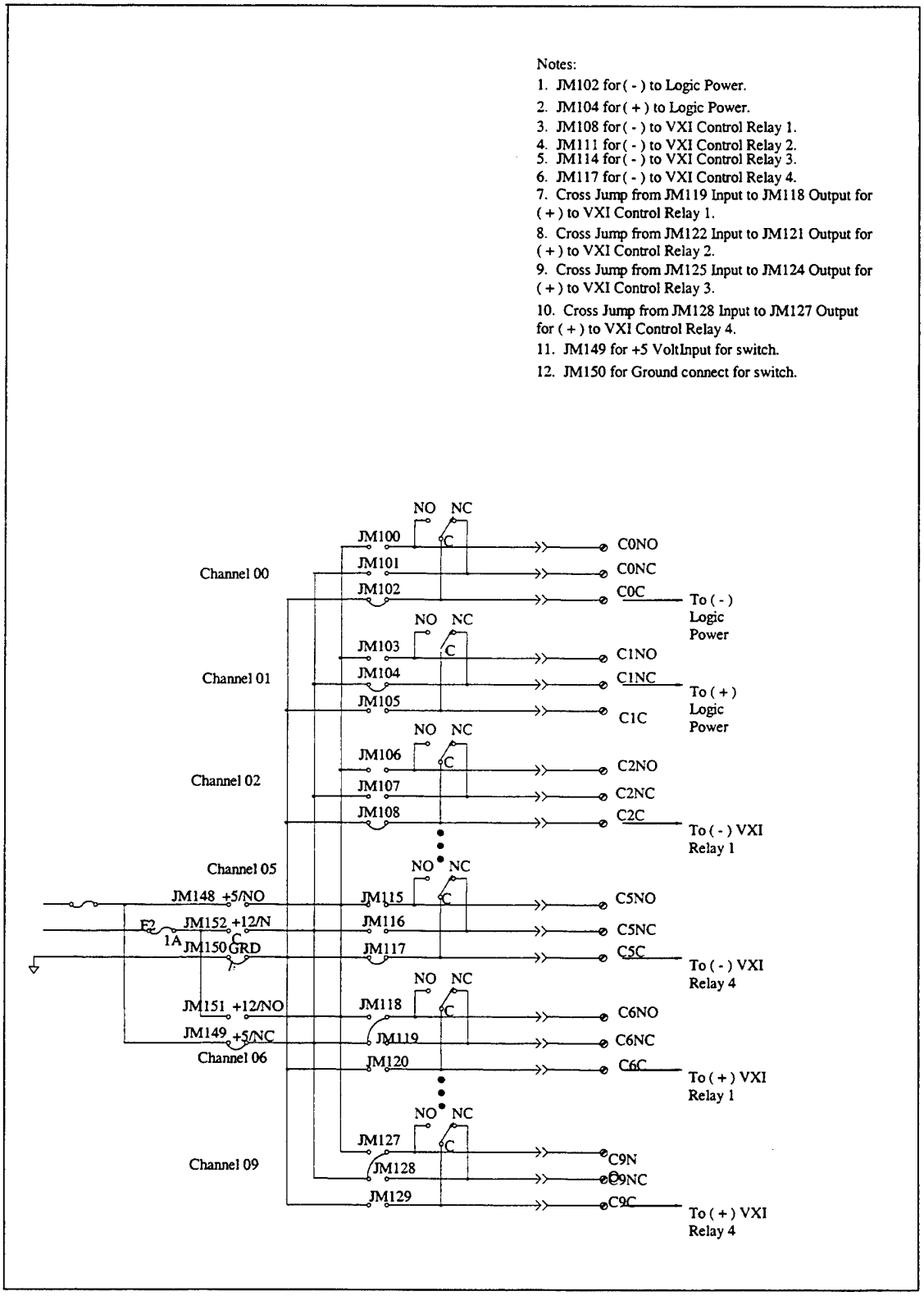

Figure 13. Wiring Diagram of Form C Switch Connections.

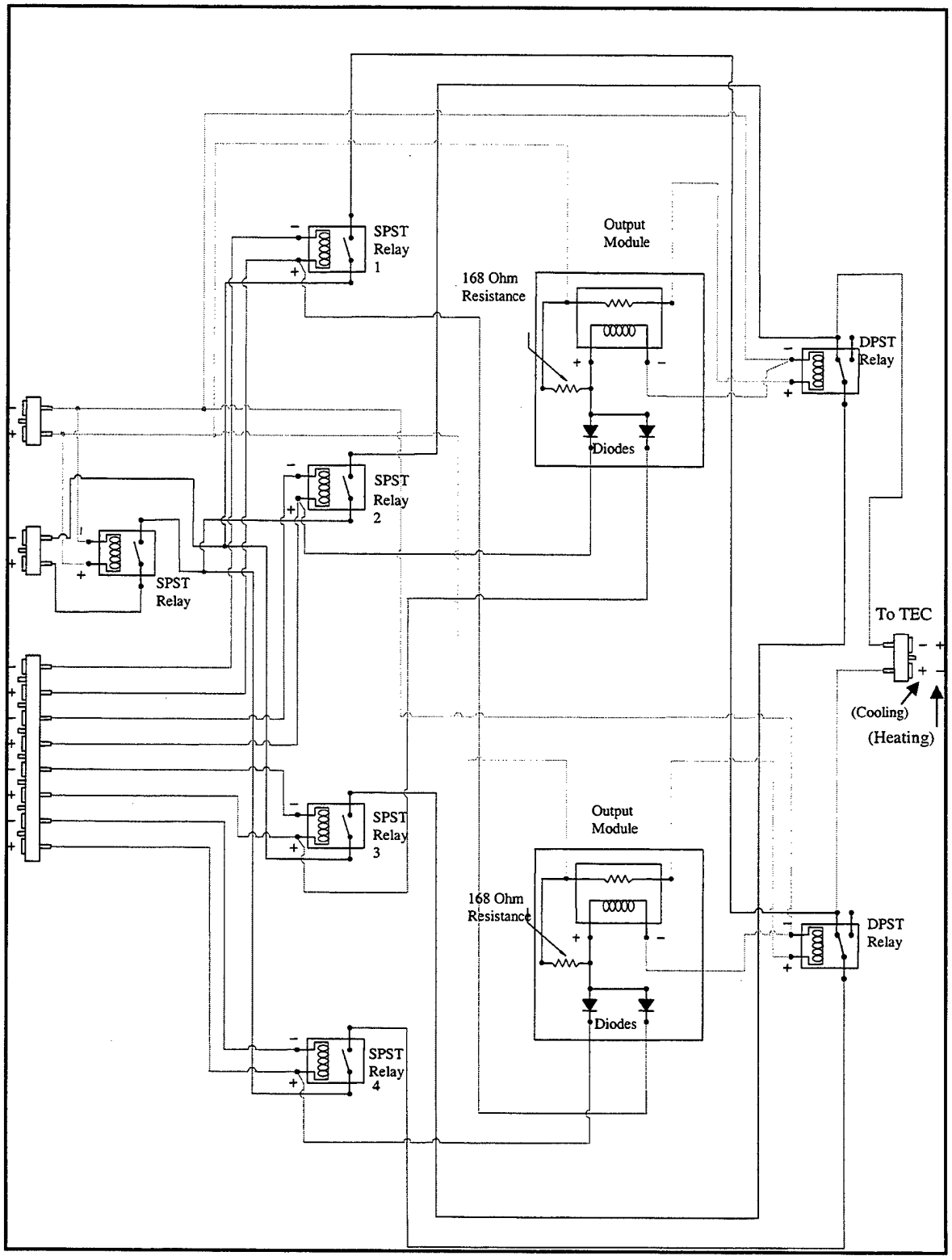

Figure 14. Wiring Diagram of the Relay Box.

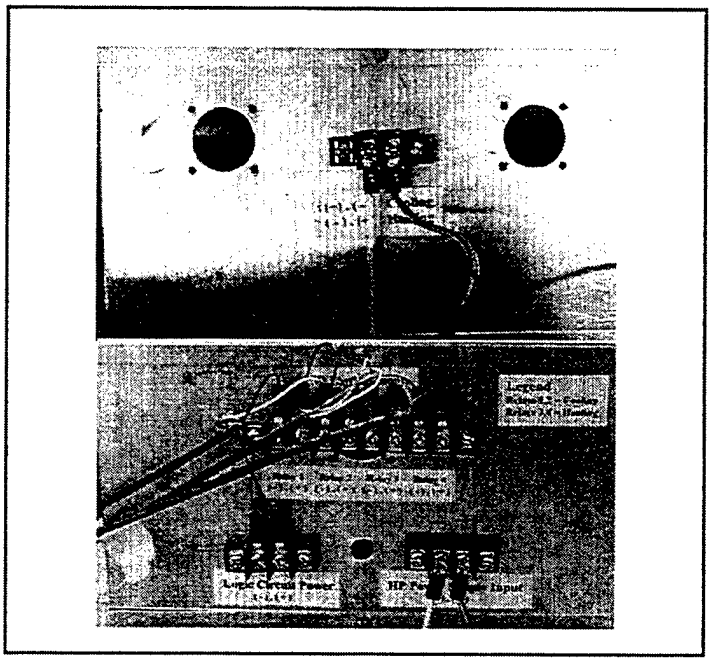

Figure 15. External Connections to the Relay Box.

D. MENSOR PCS 400 PRESSURE CALIBRATION SYSTEM

The Mensor PCS 400 Pressure Calibration System, shown in Figure 16, controlled the pressure in the chamber. The connections are shown in Figure 17. There were four ports on the back panel of the Mensor PCS 400, labeled *reference*, *measure/calibrate*, *exhaust*, and *supply*. The reference port was left open to the atmosphere; this allowed the chamber to be vented to atmospheric pressure. The measure/calibrate port was connected to the fitting in the bottom of the base of the chamber. Through this line, pressure or vacuum was applied to the chamber. The exhaust port was connected to the vacuum pump through a valve, which prevented oil from flowing from the pump to the PCS 400

when the pump was not running. The supply port was connected to a filter and then to a dry shop air supply.

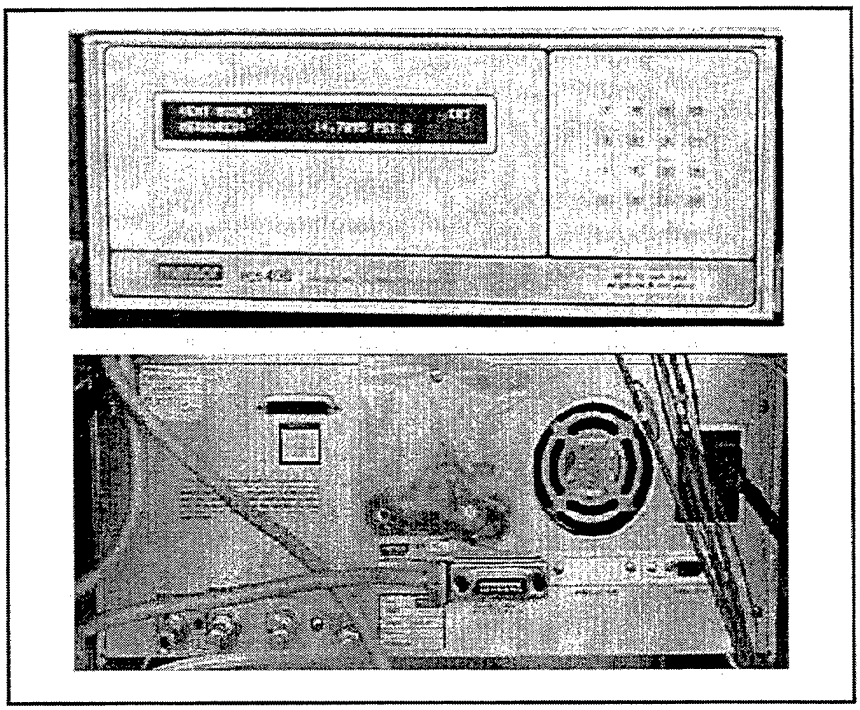

Figure 16. Mensor PCS 400 Pressure Calibration System.

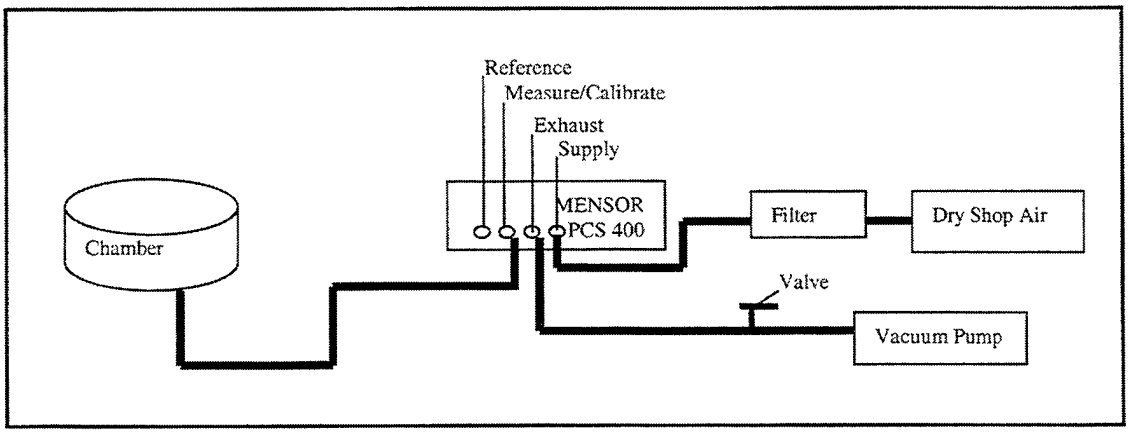

Figure 17. Schematic of the Mensor PCS 400 Connections.

E. LAMP AND PHOTO-DETECTORS

The UV illumination was provided by an Oriel Corporation 1kW quartz tungsten-halogen lamp, Model 66200, shown in Figure 18. The lamp was controlled using an Oriel Corporation controller, Model 6405, also shown in Figure 18. The tungsten-halogen incandescent source was selected for its intensity stability, despite the fact that it emitted less energy in the excitation wavelength than an arc lamp. The intensity of the light source has a direct impact on the intensity of the luminescence (see Appendix B).

Filters were used to prevent light from the lamp from entering the luminescence photodiode detector. The 380 nm excitation wavelength was chosen due to its large separation from the emission wavelength of 650 nm. An Oriel cold filter, Model 66228, and an Oriel interference filter, Model 57521, were used to isolate the light in the 380 nm range.

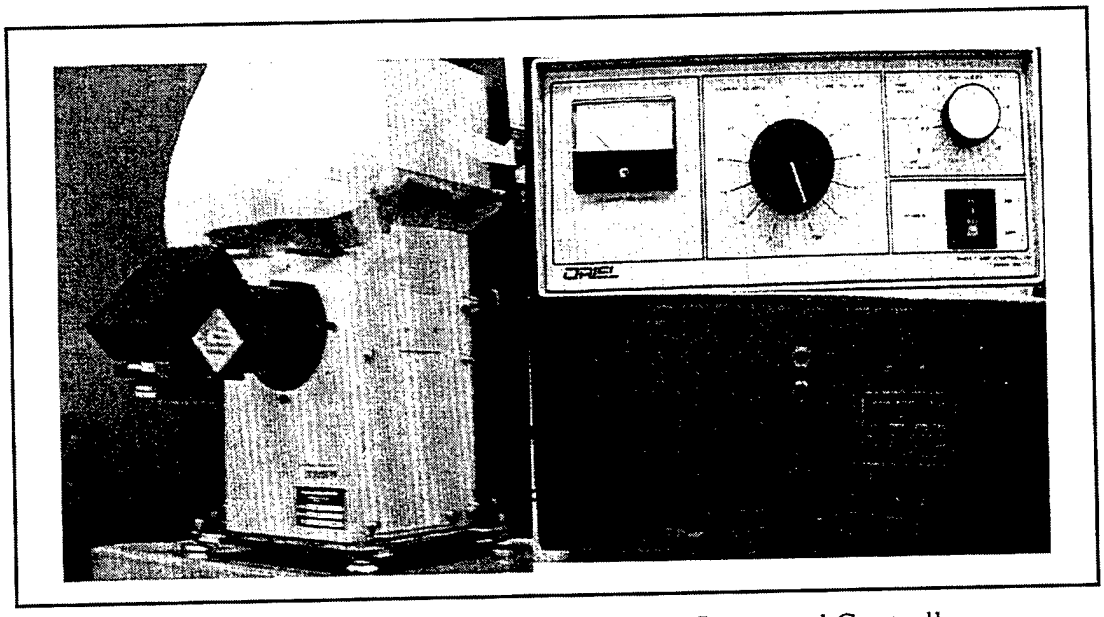

Figure 18. Oriel Model 66200 Tungsten-Halogen Lamp and Controller.

Two photodiodes were used to record intensities. One photodiode monitored the intensity of the lamp. This photodiode used no filters, since the lamp had filters blocking all frequencies except for the desired narrow band. The second diode measured the luminescent intensity of the sample. This diode had a filter, so that only the narrow band centered on the 650 nm wavelength was admitted.

Each photodiode was connected to an operational amplifier (op-amp). The wiring diagram of the photodiodes and op-amp circuit is shown in Figure 19. The output of the photodiodes was a voltage proportional to the intensity of the received light. The amplified voltage was input to an HP E1345A 16 Channel Relay Multiplexer Card, in the VXI mainframe, as shown in Figure 20. The voltage was acquired and recorded by the HP VEE program.

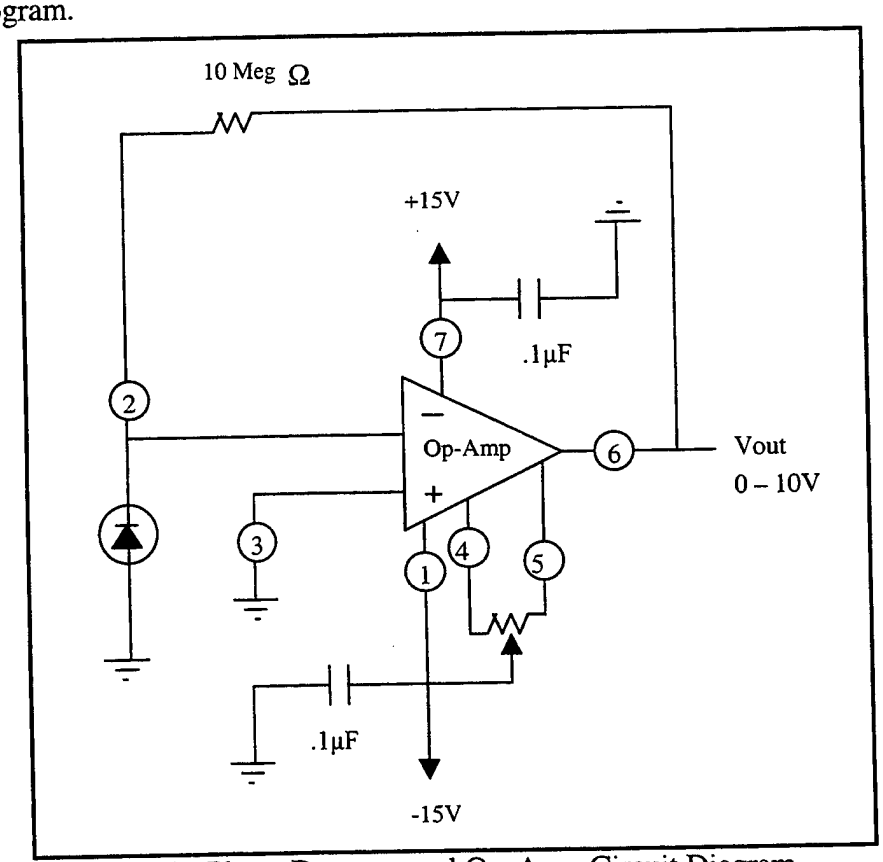

Figure 19. Photo-Detector and Op-Amp Circuit Diagram.

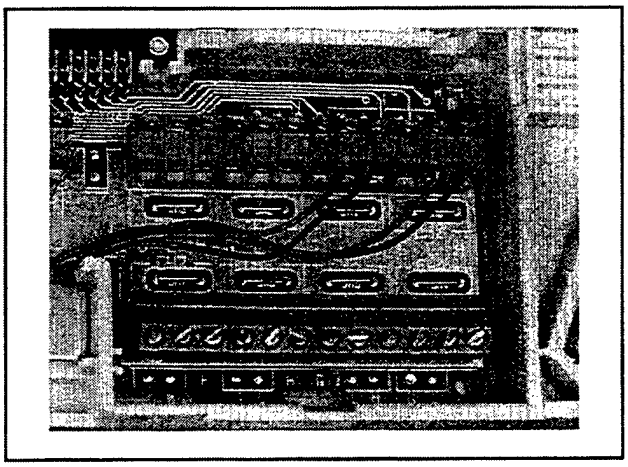

Figure 20. Wiring Diagram of 16-Channel Relay MUX Connections.

F. DATA ACQUISITION SYSTEM

The data acquisition program, ("PSP_calibration_program.vee") was written in HP VEE, running on an Inteva PC with a Pentium Processor. The program is given in Appendix C. Through the HP VEE program, the PC communicated with the VXI B-size mainframe (shown in Figure 21), Mensor PCS 400, and HP 6652A Power Supply via HPIB (IEEE 488) cables. In the listed program, the user enters the desired temperature and pressure ranges and step size. The program then sets the appropriate voltage for the desired temperature. It compares the desired temperature to the temperature of the base and sets the switches for heating or cooling. The program then waits for four minutes for the temperature of the TEC to stabilize. The program then controls the PCS 400 to set the required pressure. It then waits 30 seconds for the pressure to stabilize, then checks the temperature again. If it is not within .1° of the desired temperature, it adjusts the voltage, waits 30 seconds and checks the temperature again. Once the proper temperature

is set, the program records all channels of data necessary for the PSP calibration and moves on to the next value of temperature or pressure. The recorded data channels are identified in Table 1.

Quantity	Description	Data Acquisition Channel	Units
T_sample	Temperature of Sample	101	Degrees C
T_sink	Temperature of Base	102	Degrees C
Pressure	Commanded Pressure	Direct Input/Output	psi
I_sample	Intensity of Emission	200	volts
I_lamp	Intensity of Excitation	201	volts
Pressure_stability	Pressure stability flag	Direct Input/Output	CTRL, STABLE

Table 1. Data Acquisition Channels.

Two options were programmed. When in constant pressure mode, the program held the pressure constant while setting a range of temperatures, and then moved onto the next pressure, and ran through the temperatures again. The constant temperature mode followed the opposite sequence. The reported calibrations were conducted in the constant temperature mode.

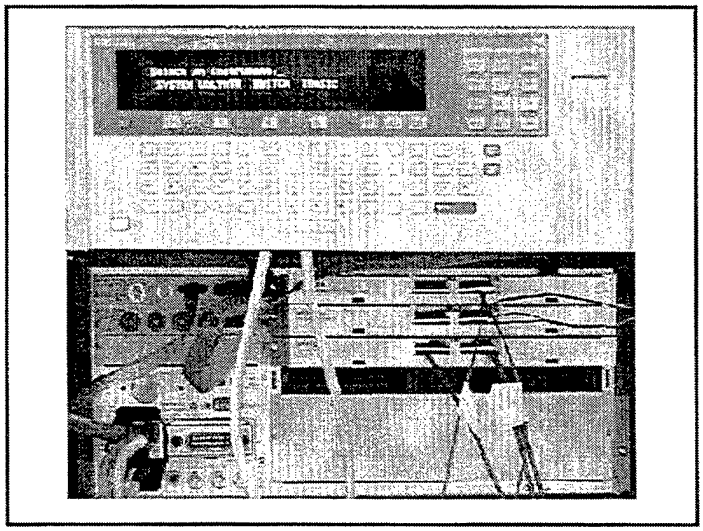

Figure 21. B-Size Mainframe.

THIS PAGE INTENTIONALLY LEFT BLANK

IV. EXPERIMENTAL PROCEDURE

A. SAMPLE PREPARATION

The aluminum coupon was cleaned with acetone to remove any paint or foreign particles that may have been on it. It was then painted with two to three coats of Krylon 1501 glossy white interior/exterior spray paint. Approximately five minutes were allowed between coats and at least three hours were allowed for the white undercoat to completely dry before applying the PSP. The white undercoat was recommended by Kavandi [Ref. 6] to reflect the light emitted off the sample and amplify the intensity of light observed. Krylon 1501 was found to have the least degradation after being exposed to PtOEP and UV light.

The PSP was then applied using an airbrush, shown in Figure 22. Nitrogen was used as the pressure source for the airbrush, as it was contaminant free. Two coats of PSP were applied, allowing approximately five minutes between coats for the paint to dry. The PSP was applied until there appeared to be a uniform coating on the entire sample. The PSP was allowed to dry for one hour, in a dark room.

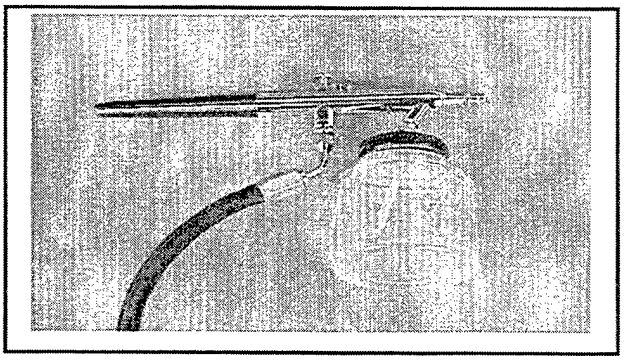

Figure 22. Airbrush Used to Apply PSP.

Once the PSP had dried, the back of the sample was cleaned with acetone, being careful not to touch the top surface of the sample as body oils could affect the response of the PSP. This ensured that no paint was inhibiting the contact between the TEC and the sample. The lens of the chamber was cleaned with plastic cleaner. The back of the sample was then coated with a thin layer of GC Electronics 10-8135 high thermal conductive heat sink compound and placed in the chamber. The chamber was positioned under the Oriel lamp and the photodiodes were positioned to measure the intensities of the sample and lamp. A piece of black poster-board was positioned around the chamber to block any ambient light from the back of the lamp and around the doors of the laboratory. After each complete temperature run, the paint would be stripped with a razor, the sample cleaned with acetone, and the process started over again. If the sample was not stripped the intensity was reduced and the results could not be used.

B. TEST PROCEDURE

The water-cooling system was turned on and allowed to run for about ten minutes to stabilize the temperature of the base. The pressure valve was opened and the vacuum pump turned on. The instruments were turned on and allowed to warm up. HP VEE was instructed to "Find Instruments," the lamp was turned on, and then the program was started. The lights and computer monitor were turned off.

The program was set to run through temperatures varying from 50° to 170° in 20° increments. At each temperature, the pressure was varied from 6.7 psi to 22.7 psi in 1 psi

increments. This includes a measurement at 14.7 psi, which is approximately atmospheric pressure. The data points were then imported into a Microsoft Excel spreadsheet.

C. DATA REDUCTION

The pressures, temperatures, and intensities had to be reduced to determine the coefficients of the analytical representation of the PSP. The derivation of the analytical representation is shown in Appendix A. The result is the following equation:

$$\frac{P}{Po} = A(Tref)\cdot F_A + B(Tref)\cdot F_B\left[\frac{Io}{I}\right] + C(T)\cdot\left[\frac{Io}{I}\right]^2 \qquad (3)$$

where F_A and F_B are quadratics in T/Tref given by Equation A6 and Equation A7.

At each pressure and temperature, ten values of intensity were recorded for the sample and ten for the lamp to minimize the effect of noise in the system. These ten values were averaged, insuring that each value was within 0.002 of the average. If a data point was outside the specified range, it was not used. The values of pressure were divided by the reference pressure, Po = 14.7 psi. The intensity values were divided into Io, the value of the intensity at Po, to obtain the ratio Io/I.

Using Microsoft Excel, a quadratic curve fit was used to determine the equation of Io/I vs. P/Po, represented by Equation A1. The A and B coefficients, so determined, were then normalized by dividing each by the corresponding A(Tref) or B(Tref) coefficient at the reference temperature, Tref. The ratioed coefficients were then plotted versus the

temperature ratio, T/Tref. A quadratic was curvefit to each of these secondary plots, which represent F_A and F_B in Equations A6 and A7 respectively. C(T), the value of C at any given temperature, is always given by Equation A5.

V. RESULTS AND DISCUSSION

A. CALIBRATION DATA

Data were taken at seven different temperatures, 50°, 70°, 90°, 110°, 130°, 150°, and 170°. At each temperature, the pressure was varied from 6.7 psi to 22.7 psi. Several of the temperatures were run a number of times to validate the repeatability of the calibration as well as to improve results that did not follow the expected pattern. These results are plotted in Appendix D.

The results of several runs did not appear to be accurate, as explained in Appendix E, so they were not used for the calibration. The data that were used for the calibration are shown in Figure 23.

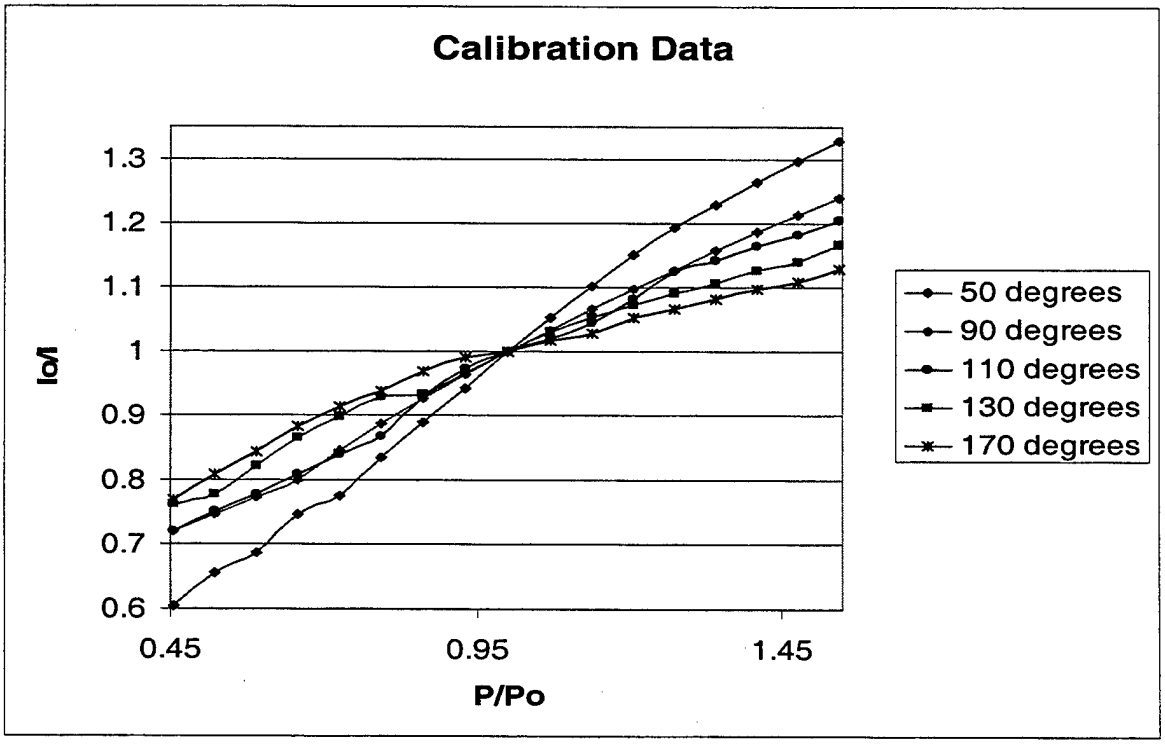

Figure 23. Calibration Data.

While some portions of the data were quite smooth other portions had significant irregularity. The irregularity may have been due to electrical noise during acquisition. Another possibility was that the white undercoat or PSP may not have been completely dry when the test was started. This might explain the runs where the first several data points were noisy and the remainder were smooth. A third possibility was that there was a temperature gradient across the aluminum coupon. This would have caused different intensities to appear at different locations on the sample; however this did not appear to be the explanation since several of the intensity measurements that were irregular had values that could not have occurred within the available range of temperature. An error in the intensity measurements was a more logical explanation. The photodiode that monitored the lamp did not have a filter on it, so it may have been sensitive to ambient light in the range of frequencies that did not affect the PSP. If this were the case, ratioing the intensities would cause errors of the type that were observed.

B. CALIBRATION REDUCTION

The coefficients of the quadratic curve fits to the lines in Figure 23 are shown in Table 2. The coefficients, normalized to the value of intensity, Io_{ref}, at the reference temperature of 90°, are also shown (=F_A and F_B respectively). The normalized A and B coefficients are plotted in Figure 24, and the C coefficients are plotted in Figure 25. Note that the sum A+B+C is nearly equal to one, as the derivation in Appendix A requires.

Figure 26 shows the normalized intensities at atmospheric pressure at the various temperatures. The curve fits to these lines are the functions F_A, F_B, and C(T), used in Equation (3).

T	A	B	C	T/Tref	A/Aref	B/Bref	Io at Po	Io/Ioref	A+B+C
50	0.1958	0.9065	-0.1055	0.555556	0.462556	1.399352	9.195375	0.560992	0.9968
90	0.4233	0.6478	-0.0755	1	1	1	16.39129	1	0.9956
110	0.4695	0.6026	-0.0778	1.222222	1.109142	0.930225	13.42835	0.819237	0.9943
130	0.4828	0.6667	-0.1477	1.444444	1.140562	1.029176	9.64632	0.588503	1.0018
170	0.5211	0.643	-0.1635	1.888889	1.231042	0.99259	6.573863	0.401058	1.0006

Table 2. Calibration Coefficients.

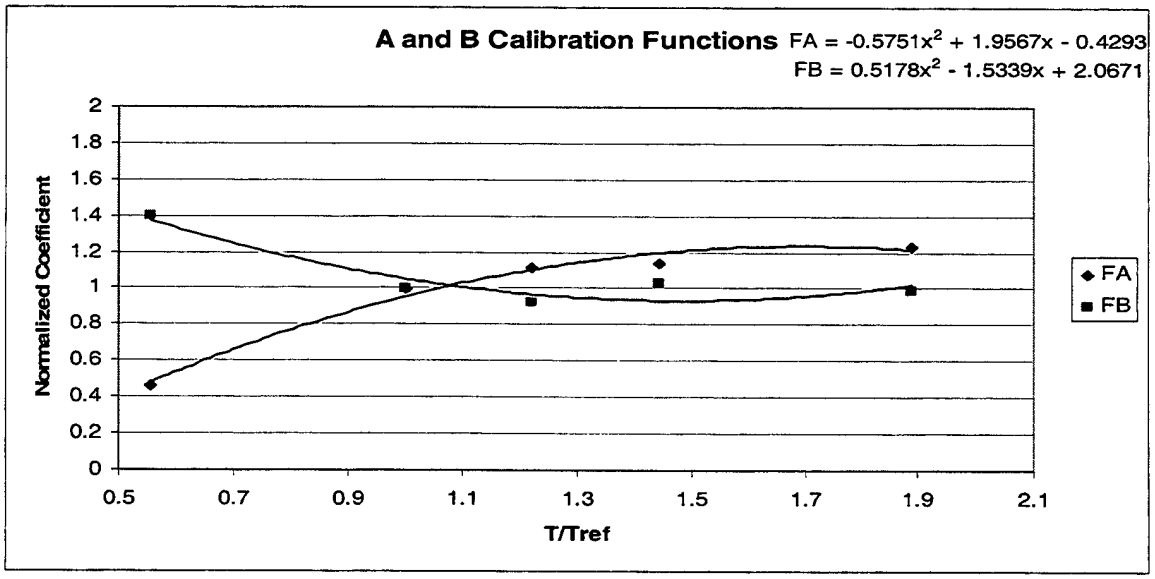

Figure 24. Calibration Functions F_A and F_B.

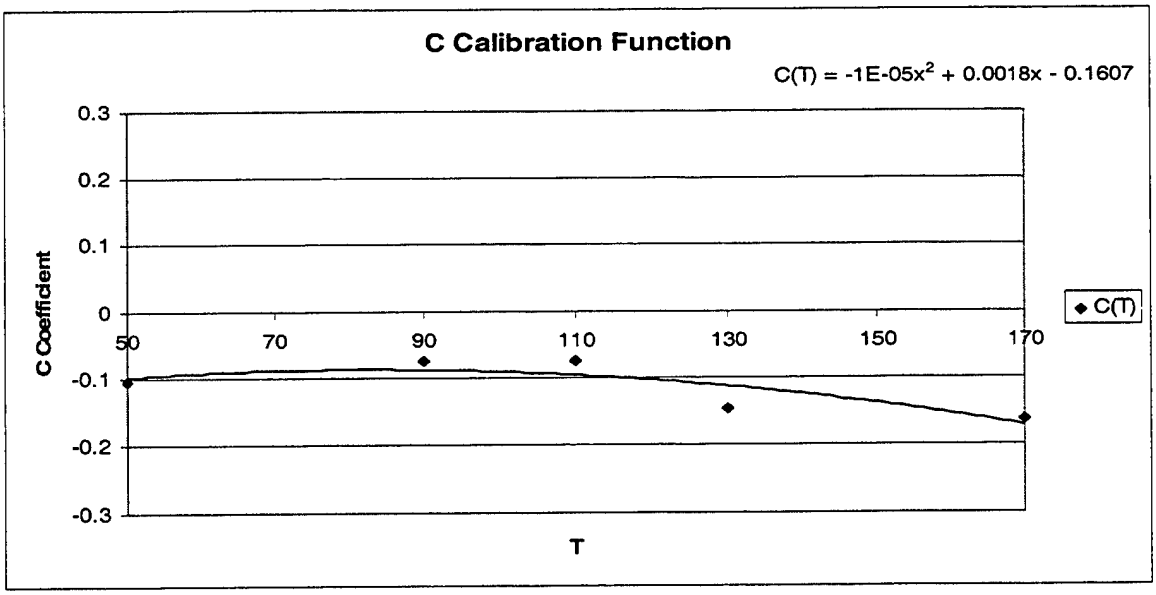

Figure 25. Calibration Function C(T).

Equation (3) was plotted using the calibration coefficients and the values of pressure and temperature that had been run. The results are shown in Figure 26. Figure 27 shows the calibration curves overlaid on the actual data points and curvefits that were used.

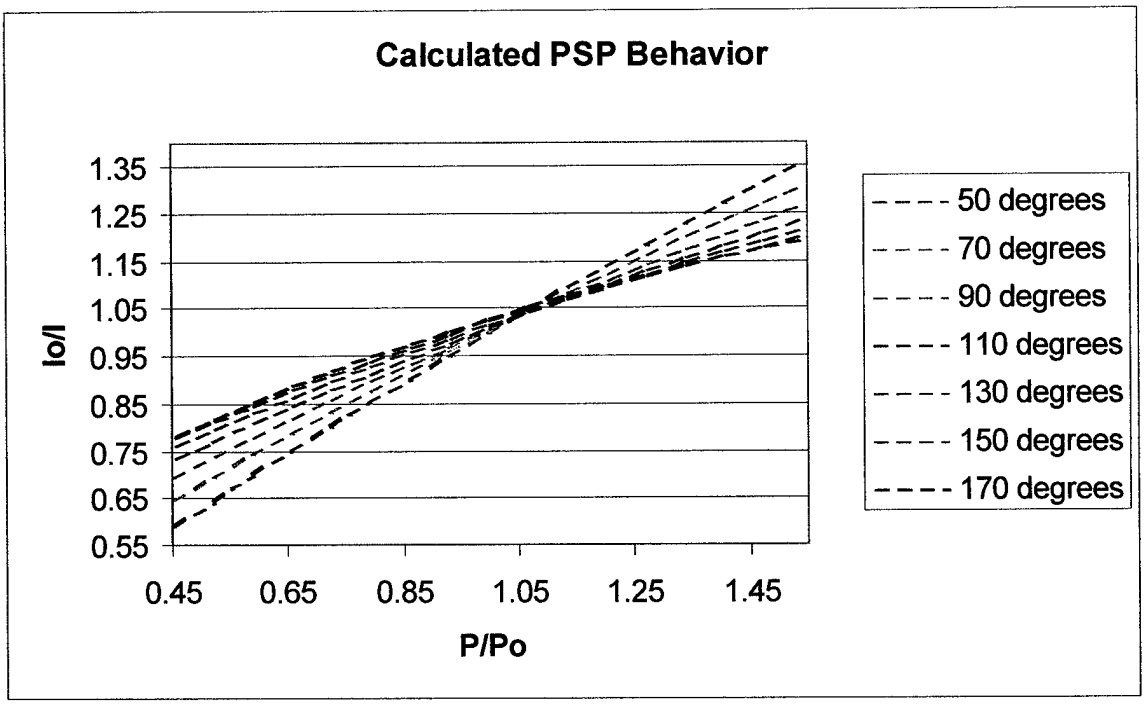

Figure 26. Calculated Pressure, Temperature, Intensity Relationship.

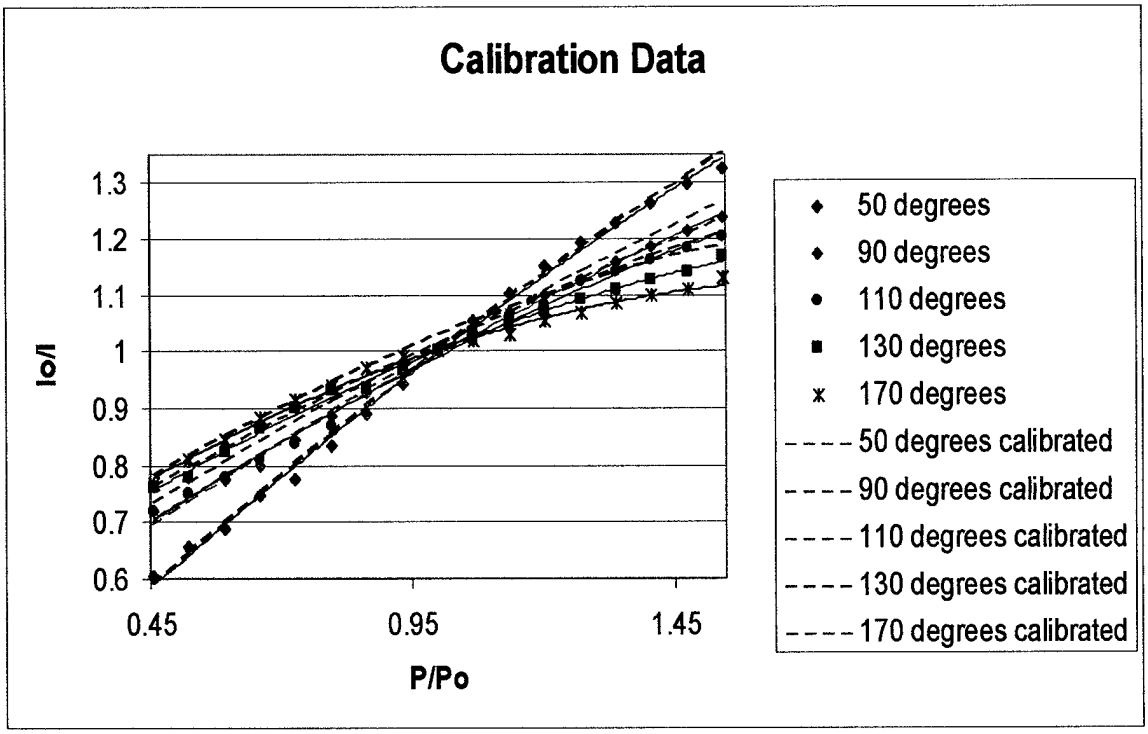

Figure 27. Calculated Curves, Data, and Curvefits to Data.

THIS PAGE INTENTIONALLY LEFT BLANK

VI. CONCLUSIONS AND RECOMMENDATIONS

A. CONCLUSIONS

A PSP calibration system was built and successfully put into operation. A first complete set of data were obtained and used to calculate an analytical representation of the PSP response. It was found that care must be taken to allow the paint to dry thoroughly before beginning calibration and to seal out all ambient light. Refinements can easily be made to eliminate variability between runs. (Possible steps are discussed in the following section.) The present data were sufficient to demonstrate that the response of the paint can be properly represented by the quadratic equations. Therefore, it should be possible to obtain quantitative measurements using two different paints, once the paints are calibrated.

PtOEP is extremely sensitive to temperature and suffers photodegradation. It does not appear to be a good choice for compressor rotor tests.

B. RECOMMENDATIONS

Small modifications to the calibration apparatus and methods should be made to improve the quality and consistency of the data. The following are suggested:

- Isolate the system (in an enclosure) to block all unnecessary light.

- Add a filter to the photodiode that monitors the lamp to isolate the intensity of the excitation frequency band.
- Fix the position of the photodiodes.
- Verify by measurements that the sample temperature is uniform.
- Repeat the procedure described in Appendix B to verify that the sample intensity is proportional to the lamp intensity, as lamp intensity varies.
- Make changes to the calibration program to improve speed and efficiency. (Currently the program terminates if a negative voltage is calculated to be necessary to adjust the temperature of the sample. The correction is to change the switch direction and send the absolute value of the voltage.)

Finally, the examination of alternate paints is recommended. A paint is required that gives greater intensity at higher temperatures. Also, the use of a PSP that is less subject to photodegradation would allow a complete calibration to be carried out without removing the sample from the chamber.

APPENDIX A. ANALYTICAL REPRESENTATION

The analytical representation of the PSP used here was a modification of that derived by Shreeve [Ref. 9]. Baumann [Ref. 4] includes a discussion of the calibration and application method proposed by Shreeve.

A quadratic form of the Stern-Volmer Equation is assumed:

$$\frac{I_0}{I} = A + B\frac{P}{P_0} + C\left[\frac{P}{P_0}\right]^2 \tag{A1}$$

where A = A(T), B = B(T), and C= C(T) and the definition of Io requires that

$$A + B + C = 1 \tag{A2}$$

The coefficients, A, B and C, must be established through calibration. The temperature dependence of the coefficients can be written as

$$\frac{A(T)}{A(Tref)} = F_A\left(\frac{T}{Tref}\right) \tag{A3}$$

$$\frac{B(T)}{B(Tref)} = F_B\left(\frac{T}{Tref}\right) \tag{A4}$$

and, always

$$C(T) = 1 - A - B \tag{A5}$$

F_A and F_B are assumed to be given by

$$F_A\left(\frac{T}{Tref}\right) = a_A + b_A\left(\frac{T}{Tref}\right) + c_A\left(\frac{T}{Tref}\right)^2 \tag{A6}$$

and

$$F_B\left(\frac{T}{Tref}\right) = a_B + b_B\left(\frac{T}{Tref}\right) + c_B\left(\frac{T}{Tref}\right)^2 \tag{A7}$$

The functions F_A and F_B can be obtained by first running the calibration acquisition program for several constant temperatures and varying pressures. The intensity data are normalized to conditions at Po (1 atmosphere), and then plotted and a quadratic curve is fit to the data. The coefficients of the curves (A, B and C) are plotted versus T/Tref and a quadratic function is curvefit to them. These curvefits represent the functions F_A and F_B. C(T) can be found either by the above method, or by subtracting A and B from 1. The functions can be substituted back into Equation (A1) to yield:

$$\frac{Io}{I} = A(Tref)\cdot F_A + B(Tref)\cdot F_B\left[\frac{P}{Po}\right] + C(T)\cdot\left[\frac{P}{Po}\right]^2 \tag{A8}$$

This equation can then be used to calculate values of intensity for a given pressure and temperature.

[It should be noted that, in the approach described in Baumann [Ref. 4], the quadratic equation assumed for the response of the paint was deliberately inverted so that the form of the calibration is then suitable for the application. The following equation is used:

$$\frac{P}{Po} = A(Tref)\cdot F_A + B(Tref)\cdot F_B\left[\frac{Io(To)}{I(T)}\cdot\frac{Io(T)}{Io(To)}\right] + C(T)\cdot\left[\frac{Io(To)}{I(T)}\cdot\frac{Io(T)}{Io(To)}\right]^2 \qquad \text{(A9)}$$

The value of Io at atmospheric pressure, Po, and varying temperature is normalized by dividing by the value of Io at the reference temperature and atmospheric pressure, giving F_I = Io(To)/Io(Tref). A quadratic curve is fit to this data to give the coefficients in

$$F_I\left(\frac{To}{Tref}\right) = a_I + b_I\left(\frac{To}{Tref}\right) + c_I\left(\frac{To}{Tref}\right)^2 \qquad \text{(A10)}$$

In the present work, the coefficients in Equation A10 were also derived from the calibration data.]

THIS PAGE INTENTIONALLY LEFT BLANK

APPENDIX B. INTENSITY CORRELATION

An experiment was conducted to see if the intensity emitted by the sample was affected by the intensity of the excitation. The lamp intensity was varied, with the chamber pressure and sample temperature constant, and the intensities of the lamp and sample were recorded. Since the sample intensity values were much smaller in magnitude than the lamp intensity values, the voltages were normalized. Each lamp intensity value was divided by the maximum lamp intensity recorded. The system recorded a baseline sample intensity when the lamp was off. This baseline voltage was subtracted from each sample intensity value to zero the sample intensity. The sample intensities were then ratioed to the sample intensity reading at the time of the maximum lamp intensity. The resulting normalized sample intensity and normalized lamp intensity are plotted in Figure B1.

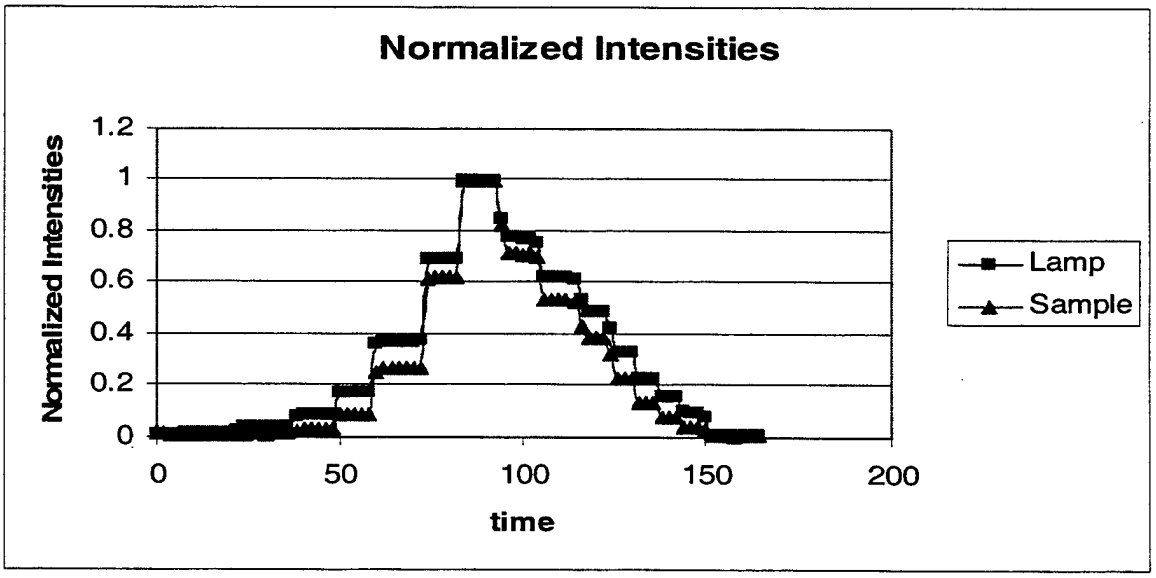

Figure B1. Normalized Lamp and Sample Intensities.

THIS PAGE INTENTIONALLY LEFT BLANK

APPENDIX C. PSP_CALIBRATION_PROGRAM

The following figures show the control/acquisition program, which was written in HPVEE. Figure C1 shows the main window. The left column shows the basic layout of the program, with all of the subroutines listed. When the start button is selected, the program goes to the check *room temperature* subroutine, shown in Figure C2. In this subroutine, the internal DVM in the mainframe measures the voltages from the thermocouples in the sample and base. The sample is on channel 1 and the base is on channel 2; the temperature of the base was considered to be room temperature. The temperature of the base is converted to degrees Fahrenheit from the Celsius reading and output from the subroutine.

The program then prompts the user to enter whether a constant temperature or pressure run is desired. Based on the user input, the program continues to the *constant pressure* or *constant temperature* subroutine. The "start, shut down chamber" portion of the main program was only used if the program was stopped mid-run. (By selecting the start switch attached to the *shut down chamber* subroutine, shown in Figure C10, the chamber was vented, the switches reset, and the power supply reset.)

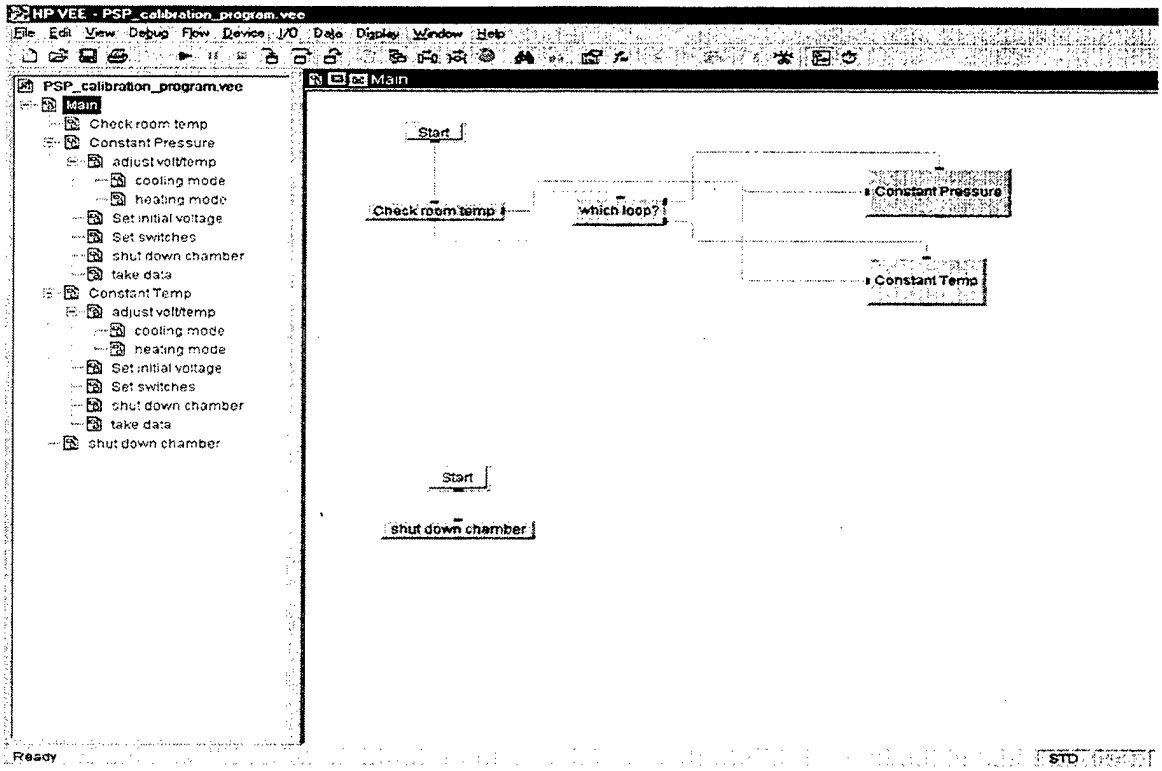

Figure C1. Main Window.

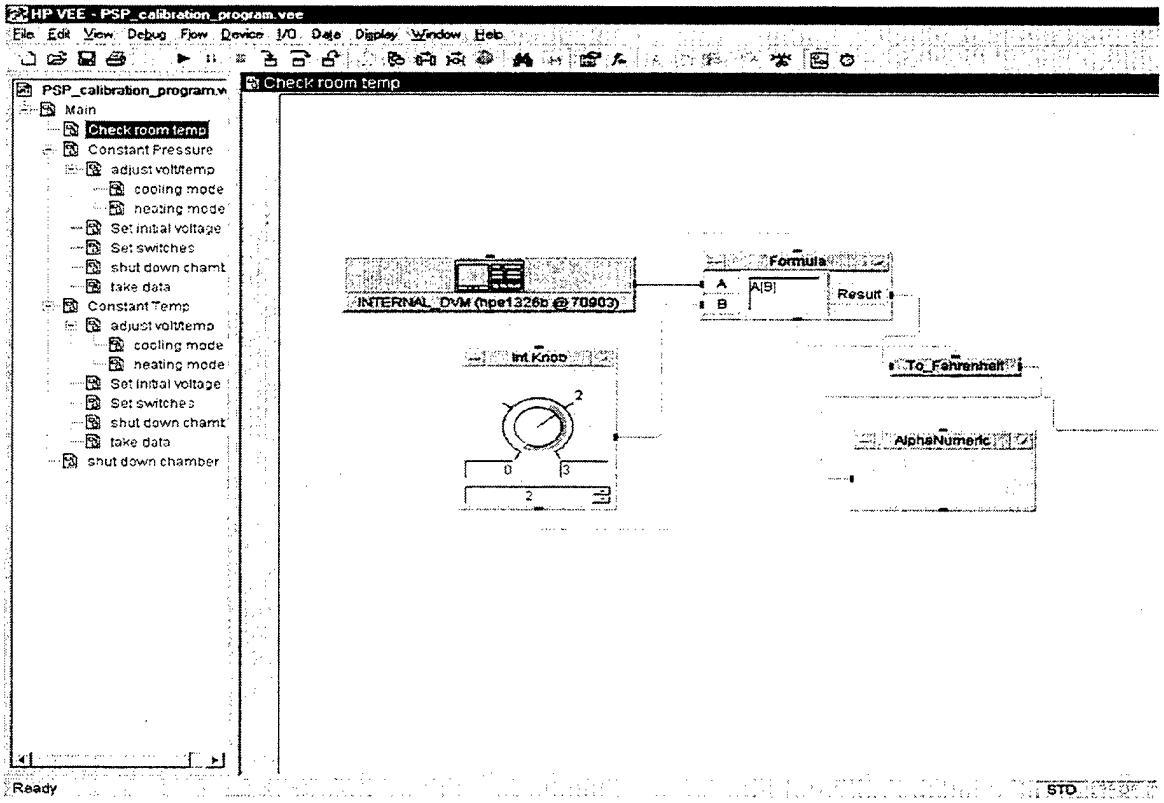

Figure C2. Check Room Temperature Subroutine.

The *constant pressure*, Figure C3, and *constant temperature*, Figure C4, subroutines each contain the same subroutines. The only difference is that they run the subroutines in a different order, to make the program more efficient for the desired range of parameters. They also group the recorded data according to which parameter is held constant to make analysis easier. The *starting pressure input*, *end pressure input*, *pressure input step size*, *starting temperature input*, *end temperature input*, and *temperature input step size* blocks prompt the user for the desired ranges of pressure and temperature for the calibration. The *until break* and *for range* blocks set up the loops. The *MENSOR_PRESS_CAL* block shows the direct input/output commands to set the pressure. *Set switches*, *set initial voltage*, *adjust voltage/temperature*, and *take data* are all subroutines. When the last run has been completed, and all the data taken, the loop is broken and the *shut down chamber* subroutine is run.

The *set switches* subroutine, shown in Figure C5, measures the temperature of the sample. It then compares the desired temperature that was input by the user, to the temperature of the sample and writes a "1" to switches 6 and 7, or 8 and 9 of the Form C Switch, depending on whether the sample needs to be heated or cooled. A "1" is also sent to the *event_enable* and *write_card* inputs to tell the computer to communicate with the Form C Switch.

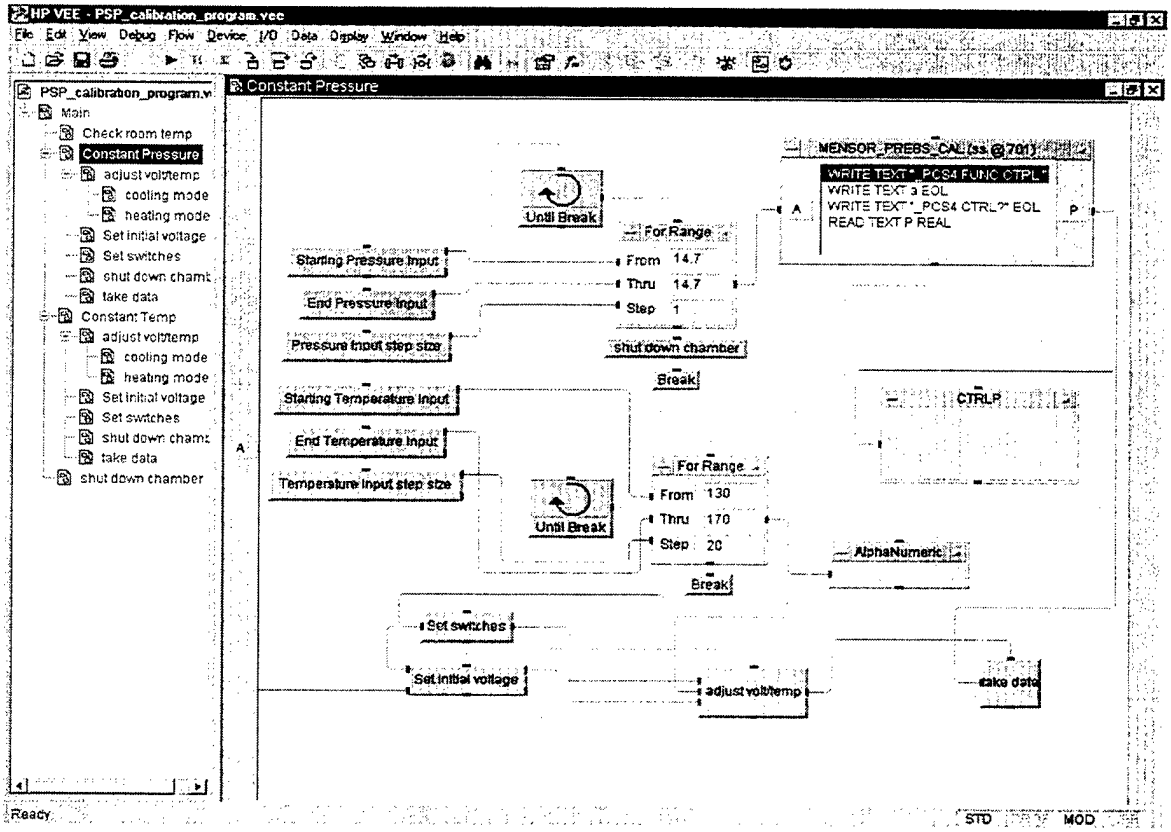

Figure C3. Constant Pressure Subroutine.

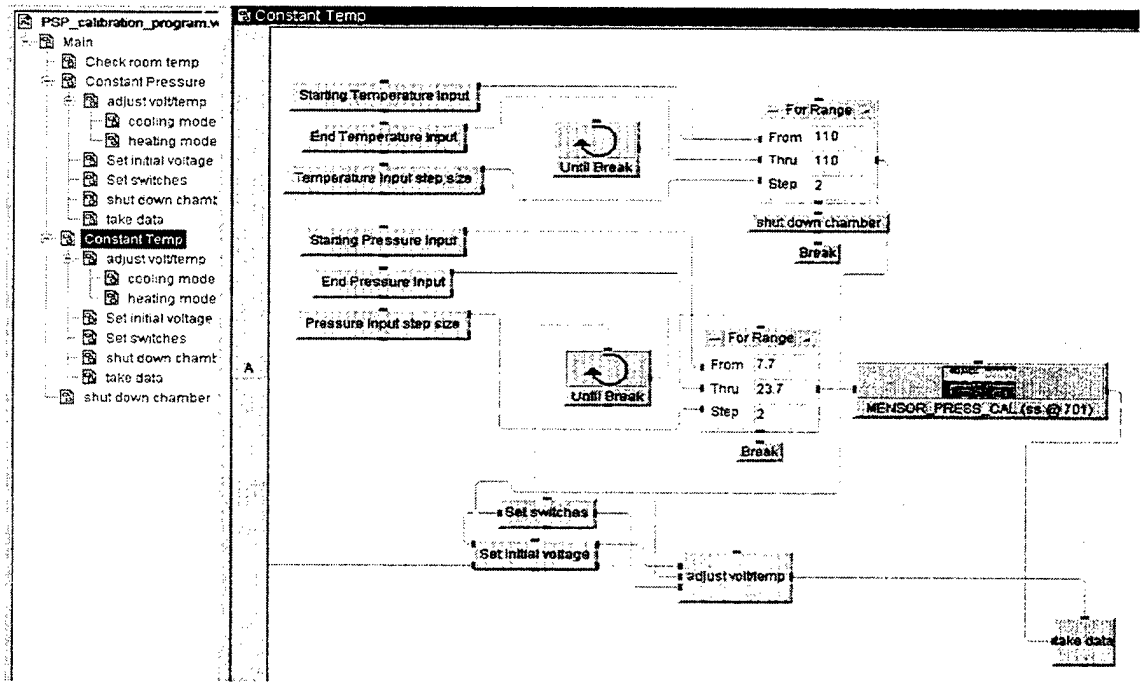

Figure C4. Constant Temperature Subroutine.

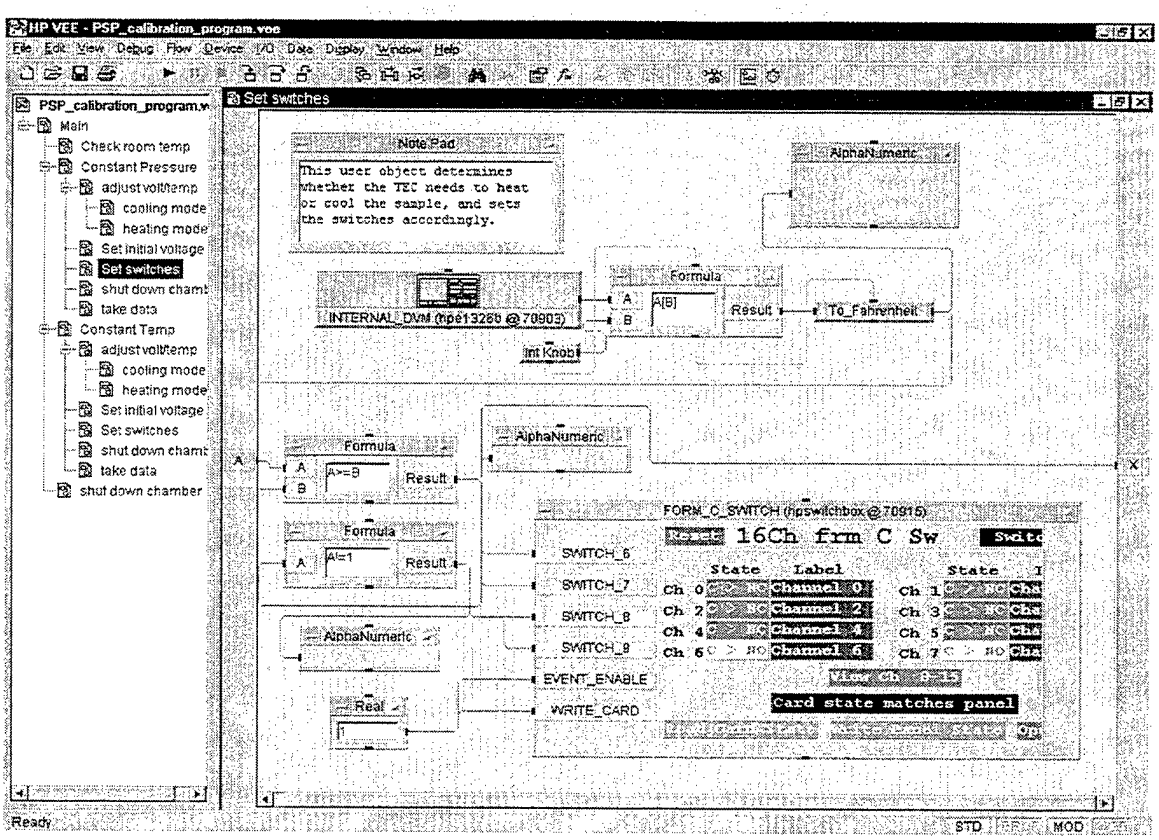

Figure C5. Set Switches Subroutine.

The *set initial voltage* subroutine, shown in Figure C6, calculates the desired temperature differential across the TEC based on the desired temperature of the sample and the temperature of the base that was recorded in the *check room temperature* subroutine. It then uses the equation of the calibration curve of the TEC, shown in Figure 16, to set a voltage. There is then a delay of four minutes to wait for the temperature of the sample to stabilize.

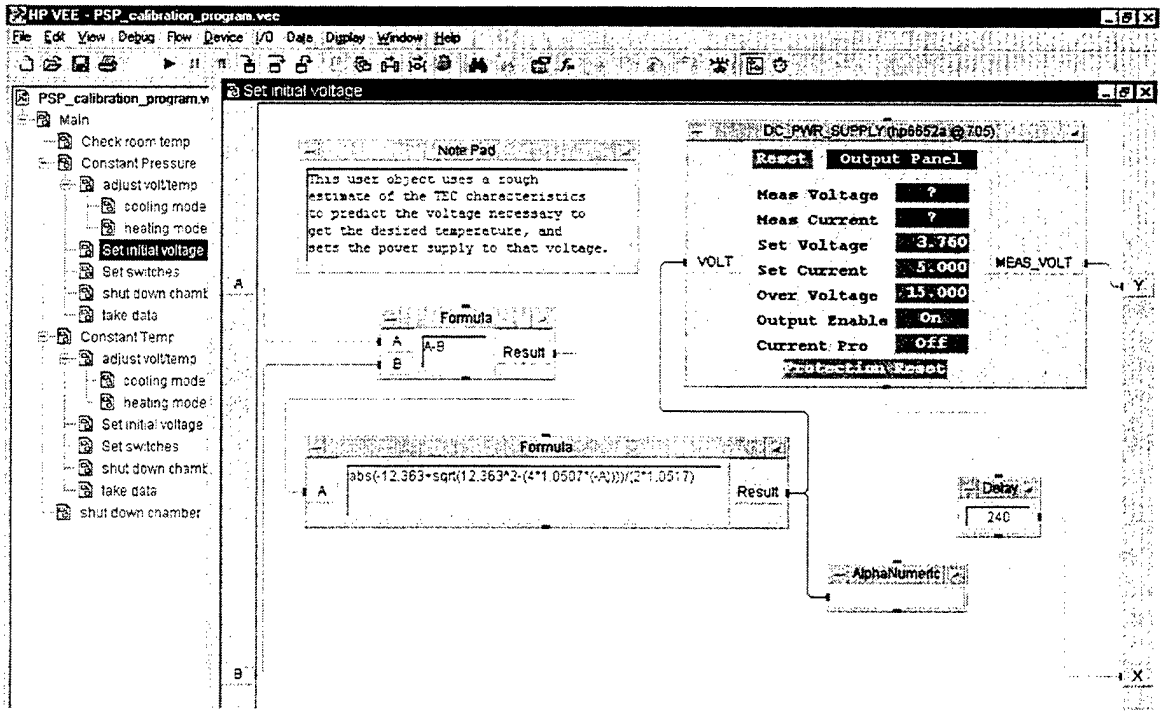

Figure C6. Set Initial Voltage Subroutine.

The *adjust voltage/temperature* subroutine, shown in Figure C7, measures the temperature of the sample and inputs it to the heating and cooling modes. Either the heating mode or cooling mode is activated depending on the whether the switches are set for heating or cooling; both will not run at the same time. The *heating mode* and *cooling mode* subroutines, shown in Figure C8, determine whether the desired temperature is within the desired range (.1°) of the desired temperature. If it is not within range, it adjusts the voltage of the power supply based on the derivative of the TEC calibration equation. It then waits 30 seconds for the temperature to be adjusted and repeats the process of checking the temperature. If it is within range, it outputs a zero which breaks the adjust voltage/temperature loop and the program moves on to take data.

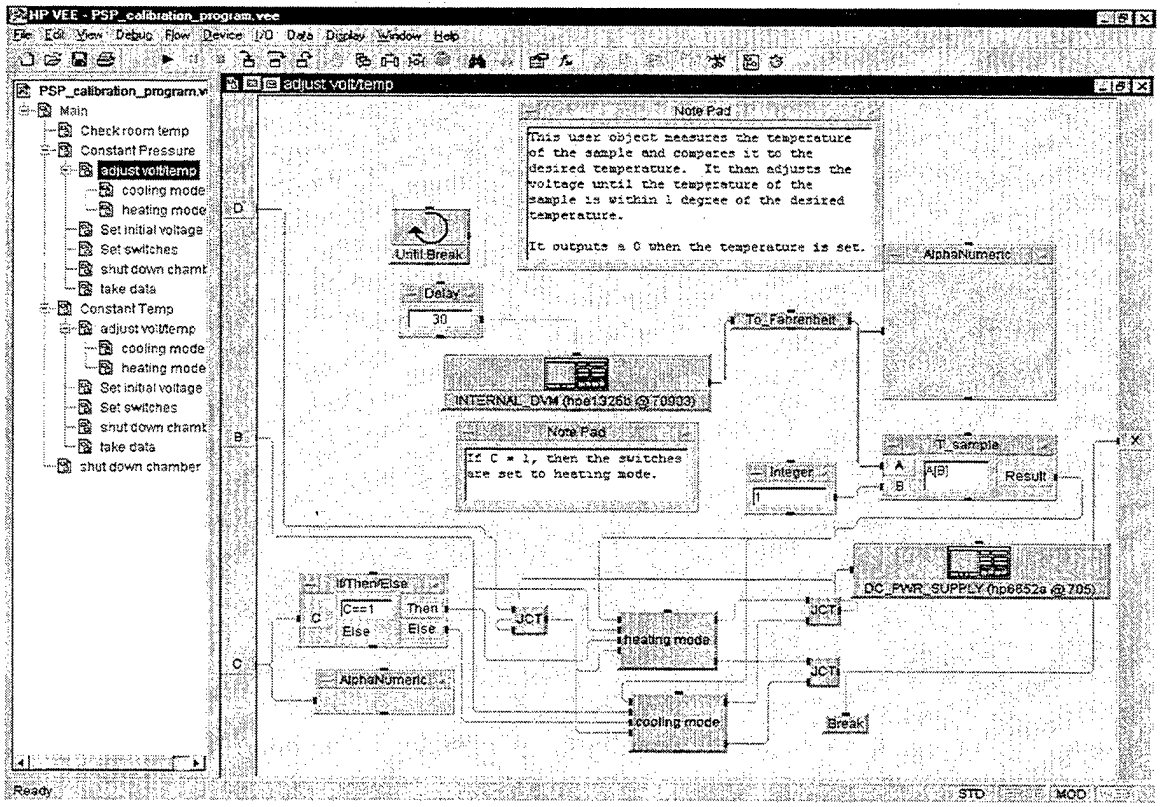

Figure C7. Adjust Voltage/Temperature Subroutine.

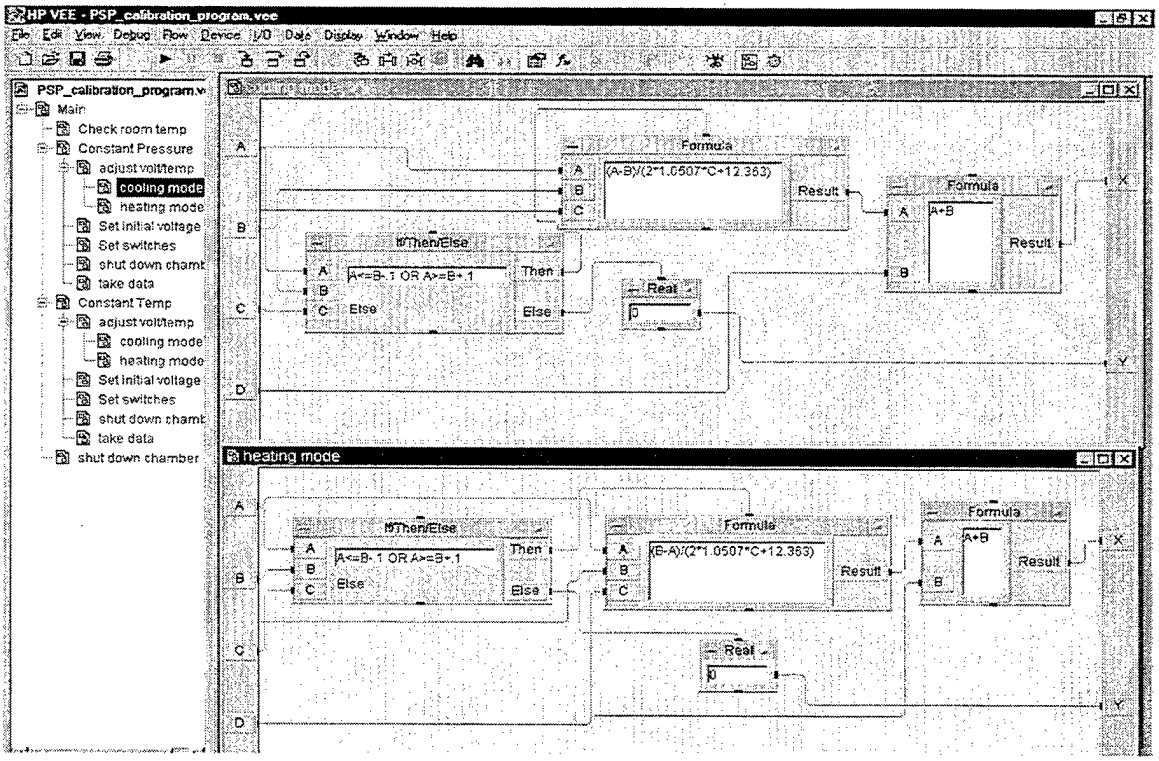

Figure C8. Cooling and Heating Mode Subroutines.

Once each pressure and temperature is satisfactorily set, the *take data subroutine*, Figure C9, runs. This subroutine records the pressure value and the stability of the pressure setting. It measures and records the temperature of the sample and base. It then takes ten readings of the intensity of the lamp and the intensity of the sample. All of the data are written to a data file called PSPdata.

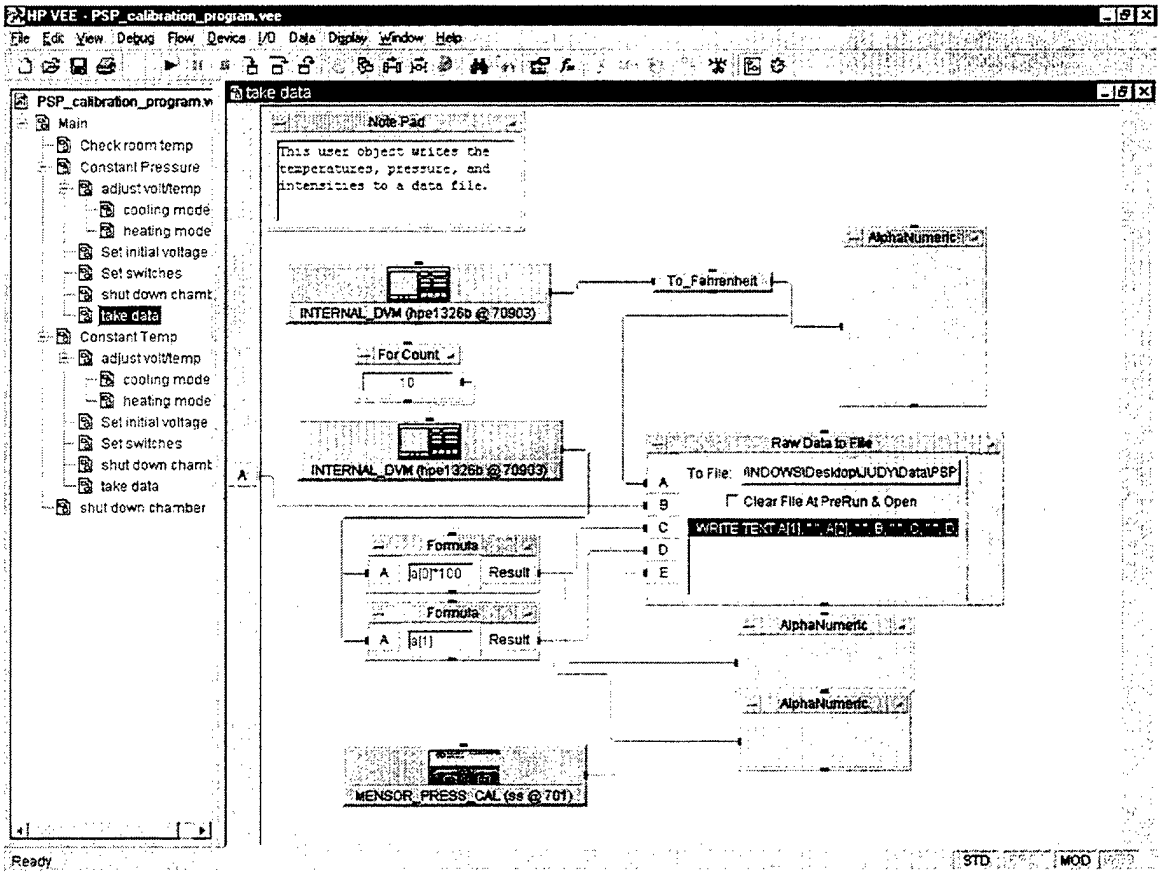

Figure C9. Take Data Subroutine.

Once all of the data have been taken, the chamber is shut down by the *shut down chamber* subroutine, Figure C10. This subroutine vents the pressure chamber to the atmosphere, and resets the switches and power supply.

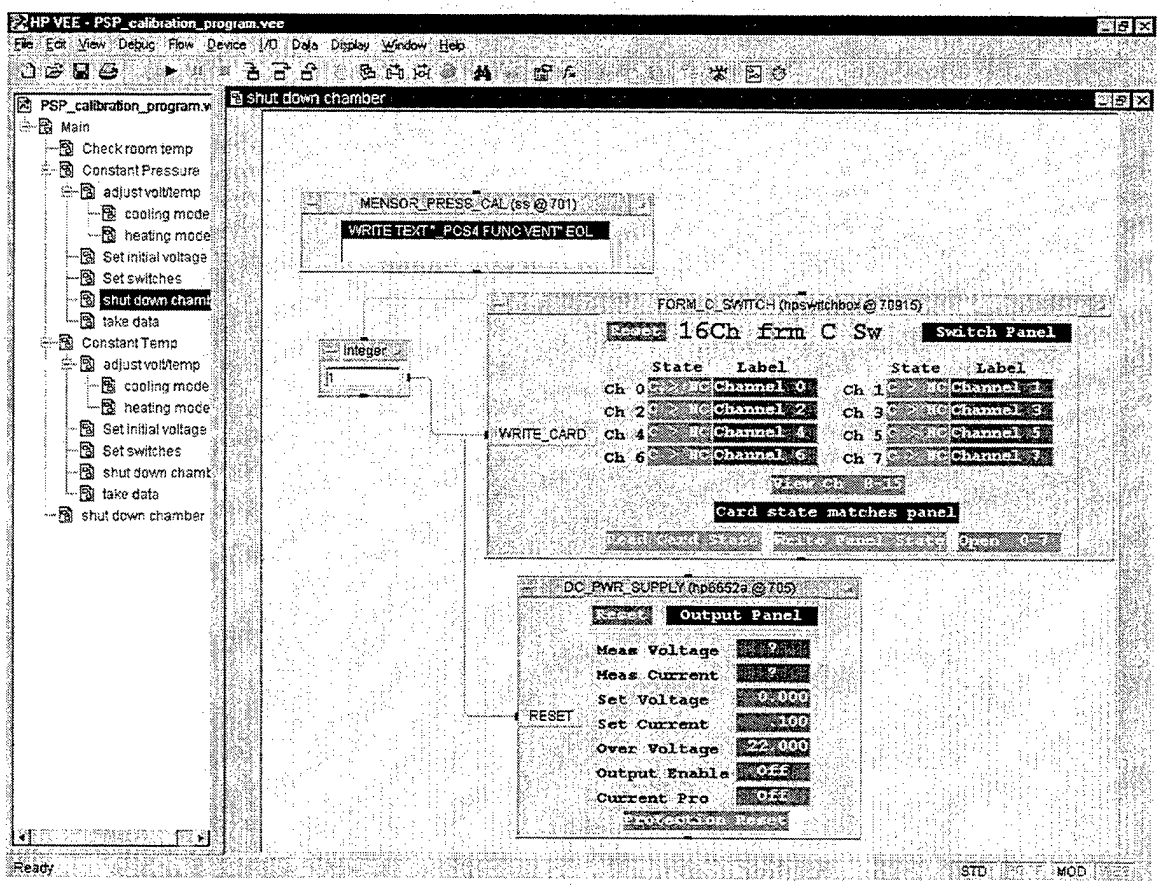

Figure C10. Shut Down Chamber Subroutine.

THIS PAGE INTENTIONALLY LEFT BLANK

APPENDIX D. DATA SETS

The following tables and plots are the data that were obtained in the present study. Each data set was taken at a constant temperature, over a range of pressures. Each average intensity is the average of ten data points. In some cases, where there was a wide range of intensities, the outlying points were neglected. The ratioed value is $\frac{Io/I}{Io/I\_lamp}$, which normalizes the intensity of the sample to changes of intensity in the lamp. Several runs were not ratioed due to inconsistent lamp intensity data; these are noted as they occur.

T_sample	T_sink	pressure	I_sample_avg	I_lamp_avg	P/Po	Io/I	Io/I_lamp	ratioed
50.14414	70.45215	6.7	15.4097271	7.95250593	0.455782	0.596725	0.987437	0.604317
50.0791	70.51895	7.7	13.7862587	7.72163696	0.52381	0.666996	1.016961	0.655872
50.17227	70.55762	8.7	13.16043854	7.71228027	0.591837	0.698713	1.018194	0.686228
50.05977	70.5875	9.7	12.04581261	7.67285767	0.659864	0.763367	1.023426	0.745894
50.17754	70.61211	10.7	11.59295082	7.67054443	0.727891	0.793187	1.023734	0.774797
50.1002	70.72285	11.7	10.84163666	7.72061768	0.795918	0.848154	1.017095	0.833898
50.11426	70.84766	12.7	10.1343441	7.69497681	0.863946	0.907348	1.020484	0.889135
50.12305	70.98477	13.7	9.648590088	7.76862793	0.931973	0.953028	1.010809	0.942837
50.11777	71.22207	14.7	9.195375443	7.8526001	1	1	1	1
50.12129	71.4998	15.7	8.633394241	7.7706604	1.068027	1.065094	1.010545	1.05398
50.10547	71.71953	16.7	8.195875883	7.71123047	1.136054	1.121952	1.018333	1.101753
50.08789	71.84258	17.7	7.946704626	7.80997925	1.204082	1.157131	1.005457	1.15085
50.12129	71.95156	18.7	7.708441019	7.84574585	1.272109	1.192897	1.000874	1.191856
50.11074	72.13965	19.7	7.436785698	7.80222778	1.340136	1.236472	1.006456	1.22854
50.12305	72.13086	20.7	7.236561775	7.80768433	1.408163	1.270683	1.005753	1.263415
50.14063	72.21875	21.7	7.051615715	7.81582642	1.47619	1.30401	1.004705	1.297903
50.11953	72.2873	22.7	6.896559	7.81514282	1.544218	1.333328	1.004793	1.326968

Table D1. Data at 50°F.

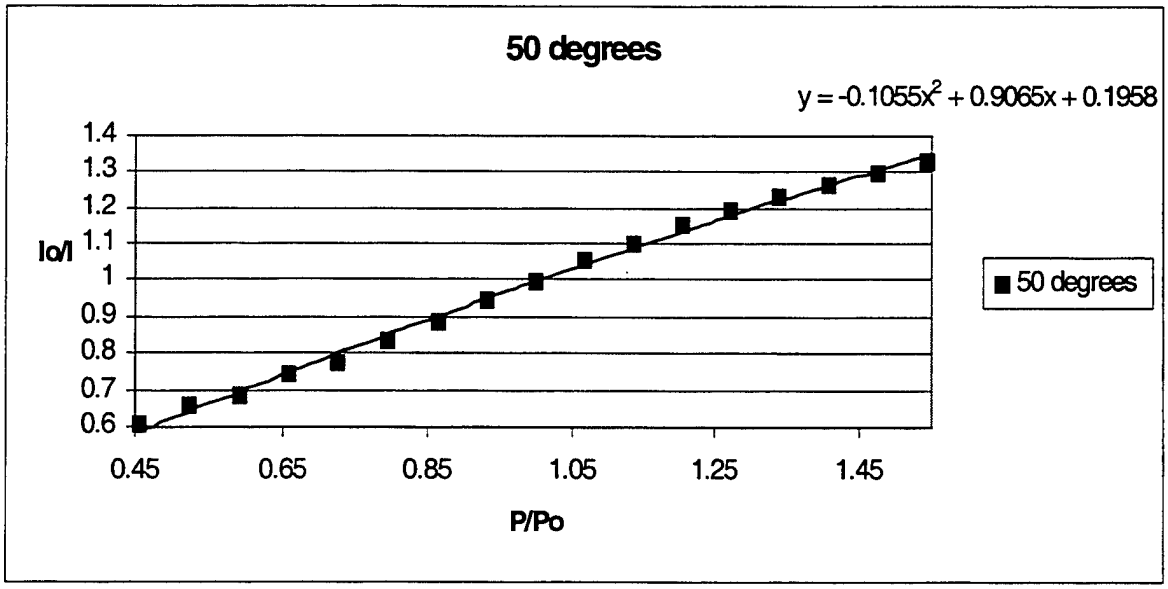

Figure D1. Plot of Ratioed Data at 50°F.

T_sample	T_sink	pressure	I_sample_avg	I_lamp_avg	P/Po	Io/I	Io/I_lamp	ratioed
69.9916	71.9832	6.7	17.6046	8.236877	0.455782	0.851482	0.985185	0.864286
70.07949	71.84082	7.7	17.2447	8.220911	0.52381	0.869252	0.987099	0.880613
70.0707	71.76875	8.7	17.0026	8.250861	0.591837	0.88163	0.983516	0.896406
70.0707	71.73711	9.7	16.57761	8.185052	0.659864	0.904232	0.991423	0.912054
70.06367	71.63164	10.7	16.25664	8.161176	0.727891	0.922085	0.994324	0.927349
69.90371	71.47871	11.7	15.89504	8.153851	0.795918	0.943061	0.995217	0.947594
69.96523	71.19746	12.7	15.4669	8.095386	0.863946	0.969166	1.002404	0.966842
69.9916	71.21152	13.7	15.23501	8.088788	0.931973	0.983917	1.003222	0.980757
69.94063	70.96895	14.7	14.99	8.11485	1	1	1	1
70.06367	71.00938	15.7	14.78099	8.115057	1.068027	1.01414	0.999974	1.014166
70.03027	70.96016	16.7	14.53959	8.093884	1.136054	1.030978	1.00259	1.028315
70.02148	70.93379	17.7	14.38661	8.118304	1.204082	1.041941	0.999574	1.042385
69.93887	70.76152	18.7	13.88827	7.972906	1.272109	1.079328	1.017803	1.060448
70.08477	70.77031	19.7	13.7016	7.96441	1.340136	1.094032	1.018889	1.07375
70.12344	70.75273	20.7	13.52815	7.961774	1.408163	1.10806	1.019226	1.087158
70.1832	70.74043	21.7	13.40253	7.982849	1.47619	1.118445	1.016536	1.100252
70.15859	70.71582	22.7	13.22825	7.97157	1.544218	1.13318	1.017974	1.113172

Table D2. Data at 70°F, Run 1.

T_sample	T_sink	pressure	I_sample_avg	I_lamp_avg	P/Po	Io/I	Io/I_lamp	ratioed
69.97051	69.13203	6.7	22.50324	9.480225	0.455782	0.818135	0.995252	0.822038
69.95293	69.20937	7.7	21.91912	9.484444	0.52381	0.839938	0.994809	0.84432
69.92832	69.32188	8.7	21.43198	9.491913	0.591837	0.859029	0.994026	0.864191
69.9459	69.37988	9.7	21.06026	9.561145	0.659864	0.874191	0.986829	0.885859
70.01797	69.43965	10.7	20.46133	9.549347	0.727891	0.89978	0.988048	0.910664
70.06895	69.53984	11.7	20.04076	9.510767	0.795918	0.918662	0.992056	0.926019
70.13574	69.61895	12.7	19.63872	9.521869	0.863946	0.937469	0.990899	0.946079
70.09707	70.1252	13.7	18.86889	9.488397	0.931973	0.975717	0.994395	0.981217
70.14453	70.21133	14.7	18.41069	9.435211	1	1	1	1

Table D3. Data at 70°F, Run 2.

T_sample	T_sink	pressure	I_sample_avg	I_lamp_avg	P/Po	Io/I	Io/I_lamp	ratioed
69.97051	71.4752	6.7	20.00009	8.270665	0.455782	0.806083	0.965661	0.834747
70.0373	71.17812	7.7	19.10978	8.157239	0.52381	0.843637	0.979088	0.861656
70.02852	71.12891	8.7	18.70996	8.154694	0.591837	0.861665	0.979394	0.879794
70.05137	71.03926	9.7	18.2085	8.148932	0.659864	0.885395	0.980086	0.903385
70.13398	71.00234	10.7	17.80321	8.139496	0.727891	0.905551	0.981223	0.922881
70.08477	70.96543	11.7	17.38285	8.117291	0.795918	0.92745	0.983907	0.94262
70.1041	70.93906	12.7	16.99243	8.099548	0.863946	0.948759	0.986062	0.96217
70.03027	70.83184	13.7	16.65253	8.089917	0.931973	0.968125	0.987236	0.980641
70.00566	70.82832	14.7	16.12172	7.986658	1	1	1	1
69.92832	70.7791	15.7	15.81322	7.977039	1.068027	1.019509	1.001206	1.018281
69.88965	70.5875	16.7	15.29375	7.917834	1.136054	1.054138	1.008692	1.045054
70.00742	70.61914	17.7	14.97787	7.890302	1.204082	1.076369	1.012212	1.063383
69.93887	70.56641	18.7	14.68046	7.869769	1.272109	1.098175	1.014853	1.082103
69.91777	70.41348	19.7	14.26654	7.875507	1.340136	1.130037	1.014114	1.11431
70.06191	70.4082	20.7	14.08281	7.89931	1.408163	1.14478	1.011058	1.13226
70.05488	70.33086	21.7	13.8889	7.914764	1.47619	1.160763	1.009083	1.150314
70.04785	70.3625	22.7	13.6631	7.904236	1.544218	1.179946	1.010428	1.167769

Table D4. Data at 70°F, Run 3.

T_sample	T_sink	pressure	I_sample_avg	I_lamp_avg	P/Po	Io/I	Io/I_lamp	ratioed
69.87383	71.13418	6.7	16.90103	5.759981	0.455782	0.72818	0.995747	0.73129
69.93887	71.12891	7.7	16.31289	5.734605	0.52381	0.754434	1.000154	0.754318
69.95645	71.04805	8.7	15.75029	5.734543	0.591837	0.781382	1.000164	0.781254
69.9125	71.06563	9.7	15.15349	5.722733	0.659864	0.812156	1.002229	0.81035
69.9582	70.82305	10.7	14.33589	5.735301	0.727891	0.858474	1.000032	0.858447
69.97578	70.79844	11.7	13.87883	5.735265	0.795918	0.886746	1.000039	0.886712
69.9793	70.80195	12.7	13.4247	5.722048	0.863946	0.916743	1.002348	0.914595
69.93711	70.75625	13.7	12.99863	5.719734	0.931973	0.946792	1.002754	0.944192
69.98809	70.65781	14.7	12.307	5.735486	1	1	1	1
70.00918	70.57871	15.7	11.94364	5.722742	1.068027	1.030423	1.002227	1.028133
70.00391	70.55762	16.7	11.57867	5.699755	1.136054	1.062903	1.006269	1.056281
70.00215	70.55234	17.7	11.25901	5.691294	1.204082	1.093079	1.007765	1.084657
70.03203	70.50313	18.7	10.98423	5.694624	1.272109	1.120424	1.007175	1.112442
69.98809	70.49609	19.7	10.69819	5.685467	1.340136	1.150381	1.008798	1.140348
69.95293	70.49082	20.7	10.4402	5.684876	1.408163	1.178809	1.008902	1.168407
69.97227	70.46094	21.7	10.24553	5.711038	1.47619	1.201206	1.004281	1.196086
69.95469	70.48027	22.7	10.01144	5.70168	1.544218	1.229293	1.005929	1.222047

Table D5. Data at 70°F, Run 4.

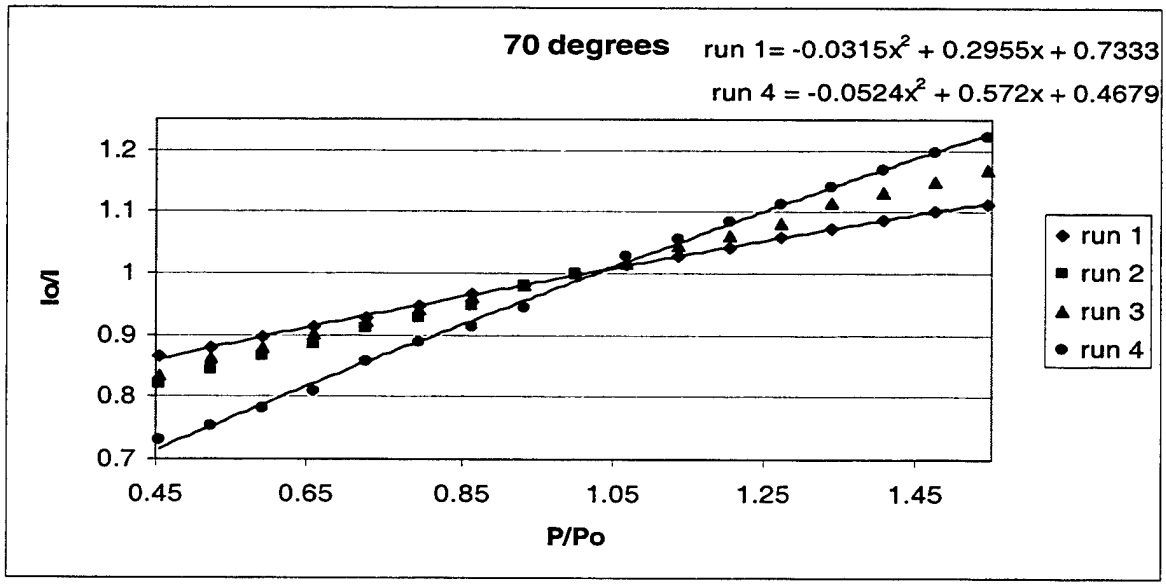

Figure D2. Plot of Ratioed Data at 70°F.

T_sample	T_sink	pressure	I_sample_avg	I_lamp_avg	P/Po	Io/I	Io/I_lamp	ratioed
89.99902	70.55762	6.7	23.41228	10.54075	0.455782	0.700115	0.973708	0.719019
90.07988	70.61914	7.7	22.57292	10.54075	0.52381	0.726148	0.973708	0.745756
90.13613	70.69121	8.7	21.72929	10.52037	0.591837	0.754341	0.975594	0.773212
90.18008	70.73164	9.7	20.91519	10.47289	0.659864	0.783702	0.980017	0.799682
90.00781	70.79141	10.7	19.62233	10.38652	0.727891	0.835339	0.988166	0.845342
90.07461	70.7334	11.7	18.6426	10.36226	0.795918	0.879238	0.99048	0.887689
90.02012	70.7123	12.7	17.74847	10.30676	0.863946	0.923532	0.995814	0.927415
90.02715	70.59102	13.7	17.0344	10.29573	0.931973	0.962246	0.996881	0.965257
90.05527	70.49434	14.7	16.39129	10.26361	1	1	1	1
89.97617	70.48203	15.7	15.8268	10.24385	1.068027	1.035667	1.001929	1.033672
90.03066	70.42578	16.7	15.2115	10.16818	1.136054	1.077559	1.009386	1.067539
90.09395	70.39414	17.7	14.93431	10.26833	1.204082	1.097559	0.99954	1.098064
90.03066	70.3959	18.7	14.67347	10.35607	1.272109	1.117069	0.991072	1.127132
90.06934	70.36426	19.7	14.25112	10.3245	1.340136	1.150176	0.994103	1.156999
90.07637	70.36602	20.7	13.89861	10.31567	1.408163	1.179347	0.994954	1.185329
90.02539	70.39941	21.7	13.57939	10.30734	1.47619	1.207071	0.995758	1.212214
90.08867	70.38887	22.7	13.2558	10.28034	1.544218	1.236537	0.998373	1.238553

Table D6. Data at 90°F.

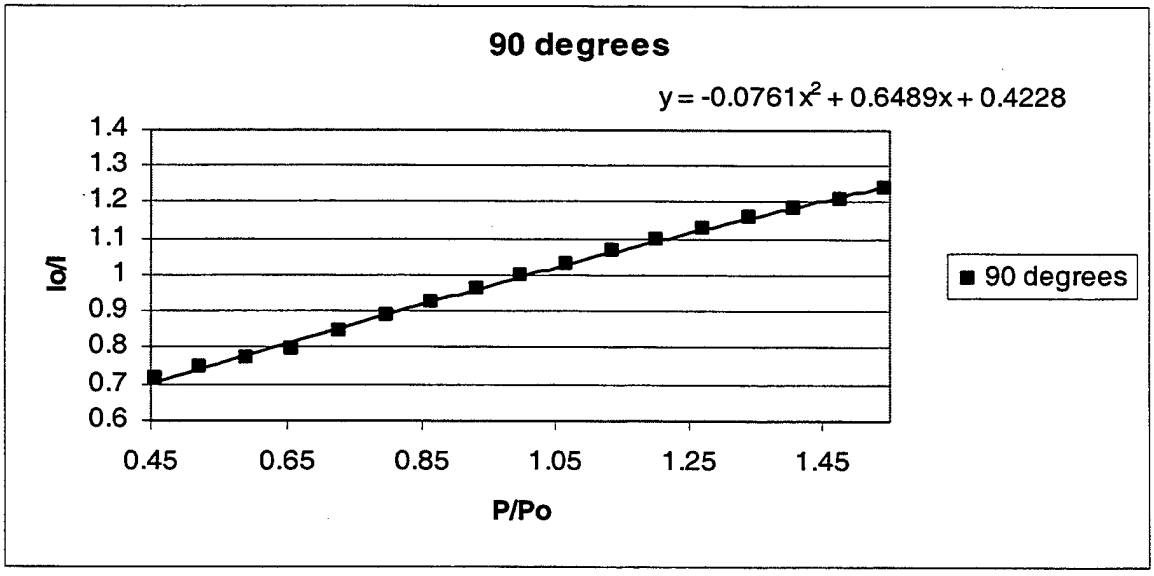

Figure D3. Plot of Ratioed Data at 90°F.

T_sample	T_sink	pressure	I_sample_avg	I_lamp_avg	P/Po	Io/I	Io/I_lamp	ratioed
109.952	70.82832	6.7	18.6924	8.274821	0.455782	0.718386	0.978356	0.734279
110.0855	70.89336	7.7	17.89669	8.296405	0.52381	0.750326	0.975811	0.768926
110.1365	70.89512	8.7	17.26503	8.319562	0.591837	0.777777	0.973095	0.799282
110.1717	70.93203	9.7	16.61202	8.304681	0.659864	0.808351	0.974838	0.829216
110.1066	70.96016	10.7	16.00804	8.27699	0.727891	0.838851	0.9781	0.857633
110.0082	70.95488	11.7	15.48682	8.232324	0.795918	0.867082	0.983407	0.881713
110.1242	71.00762	12.7	14.44246	8.078741	0.863946	0.929783	1.002102	0.927833
109.952	71.11309	13.7	13.7825	8.104303	0.931973	0.974305	0.998941	0.975337
110.0451	71.1957	14.7	13.42835	8.095721	1	1	1	1
110.0047	71.23965	15.7	13.16335	8.128369	1.068027	1.020132	0.995983	1.024246
110.0047	71.23262	16.7	12.86735	8.12558	1.136054	1.043599	0.996325	1.047448
110.1365	71.27656	17.7	12.40808	8.101178	1.204082	1.082227	0.999326	1.082956
109.9502	71.43477	18.7	11.9524	8.082428	1.272109	1.123486	1.001645	1.121641
110.0715	71.45234	19.7	11.76515	8.113269	1.340136	1.141367	0.997837	1.143841
110.1313	71.50684	20.7	11.54405	8.109192	1.408163	1.163228	0.998339	1.165163
110.1277	71.48223	21.7	11.35271	8.120746	1.47619	1.182832	0.996918	1.186489
110.0873	71.54023	22.7	11.16323	8.120428	1.544218	1.202909	0.996957	1.20658

Table D7. Data at 110°F.

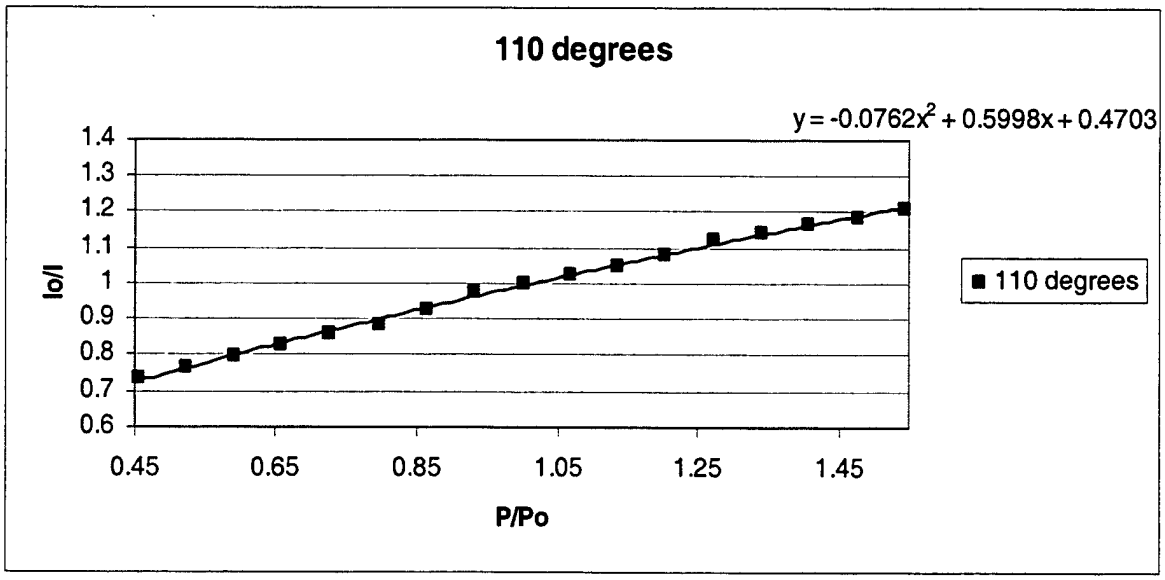

Figure D4. Plot of Ratioed Data at 110°F.

T_sample	T_sink	pressure	I_sample_avg	I_lamp_avg	P/Po	Io/I	Io/I_lamp	ratioed
129.9277	71.91465	6.7	12.8692	10.73952	0.455782	0.749567	0.985539	0.760565
130.1703	71.97266	7.7	12.34639	10.53935	0.52381	0.781307	1.004258	0.777994
130.0895	72.31016	8.7	11.70964	10.55524	0.591837	0.823793	1.002746	0.821537
129.9805	72.67051	9.7	11.45044	10.86392	0.659864	0.842441	0.974254	0.864703
129.998	72.9043	10.7	11.05432	10.90485	0.727891	0.872629	0.970597	0.899064
129.9436	73.10469	11.7	10.62843	10.85255	0.795918	0.907596	0.975275	0.930605
130.0684	73.22422	12.7	10.26213	10.51674	0.863946	0.939992	1.006417	0.933998
129.9664	73.36309	13.7	9.911089	10.51199	0.931973	0.973286	1.006871	0.966644
130.0068	73.53711	14.7	9.64632	10.58422	1	1	1	1
129.9207	73.57754	15.7	9.419203	10.66988	1.068027	1.024112	0.991972	1.0324
130.0771	73.65664	16.7	9.242153	10.68615	1.136054	1.043731	0.990462	1.053782
130.1492	73.66543	17.7	9.051819	10.65105	1.204082	1.065678	0.993726	1.072406
130.1422	73.66543	18.7	8.910875	10.65946	1.272109	1.082533	0.992942	1.090229
130.1	73.68828	19.7	8.760881	10.64774	1.340136	1.101067	0.994035	1.107675
129.9963	73.72168	20.7	8.640709	10.67062	1.408163	1.116381	0.991903	1.125493
129.9805	73.68301	21.7	8.465114	10.58051	1.47619	1.139538	1.000351	1.139138
129.9172	73.81484	22.7	8.3429	10.68452	1.544218	1.156231	0.990613	1.167187

Table D8. Data at 130°F.

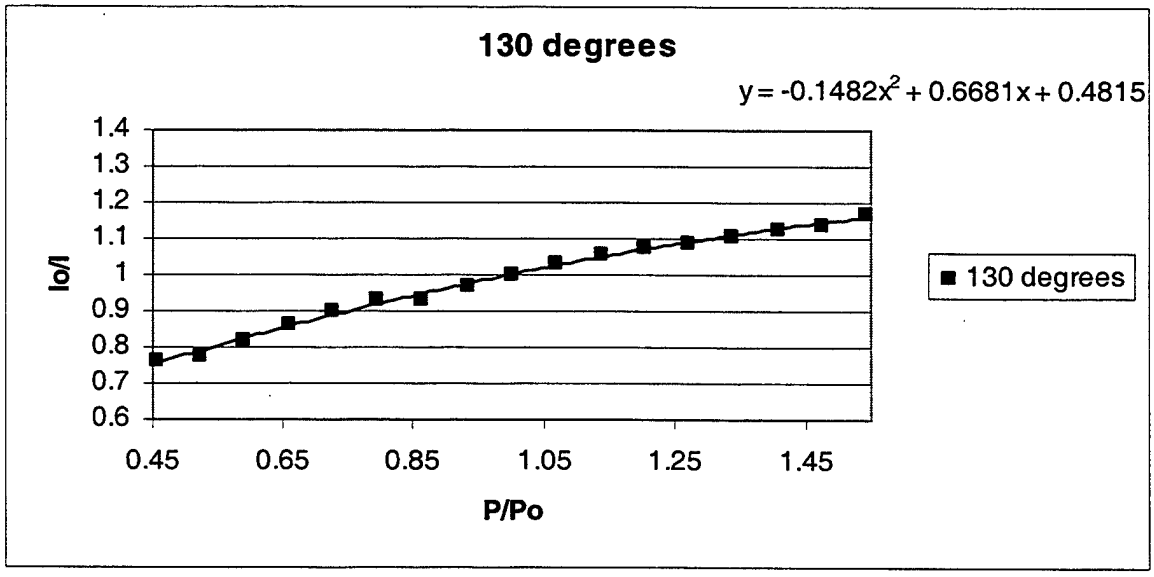

Figure D5. Plot of Ratioed Data at 130°F.

T_sample	T_sink	pressure	I_sample_avg	I_lamp_avg	P/Po	Io/I	Io/I_lamp	ratioed
150.0547	73.27168	6.7	8.579235	7.681207	0.455782	0.804716	1.13552	0.708676
150.074	73.41934	7.7	8.29466	7.691541	0.52381	0.832324	1.133995	0.733975
150.0037	73.51602	8.7	7.987574	7.689594	0.591837	0.864323	1.134282	0.762
150.074	74.95566	9.7	7.700174	7.651294	0.659864	0.896583	1.13996	0.786504
149.9721	75.0875	10.7	7.456381	7.675171	0.727891	0.925898	1.136414	0.814754
150.0301	75.79941	11.7	7.247019	8.597906	0.795918	0.952646	1.014453	0.939074
149.9316	75.83457	12.7	7.210662	8.678815	0.863946	0.957449	1.004995	0.952691
150.1391	76.00332	13.7	7.119569	8.739563	0.931973	0.9697	0.99801	0.971634
150.009	76.08418	14.7	6.903845	8.722168	1	1	1	1
150.0301	76.30039	15.7	6.915085	7.86748	1.068027	0.998375	1.108635	0.900544
149.9791	76.34609	16.7	6.791464	7.883221	1.136054	1.016547	1.106422	0.91877
150.1074	76.55703	17.7	6.533152	7.808356	1.204082	1.05674	1.11703	0.946027
150.0213	76.54297	18.7	6.509235	7.754547	1.272109	1.060623	1.124781	0.94296
149.9633	76.71172	19.7	6.463577	8.719324	1.340136	1.068115	1.000326	1.067767
150.0248	76.84355	20.7	6.344407	8.054645	1.408163	1.088178	1.082874	1.004898
150.0178	76.91563	21.7	6.193824	8.049854	1.47619	1.114634	1.083519	1.028717
150.06	77.06328	22.7	6.148814	8.118176	1.544218	1.122793	1.0744	1.045042

Table D9. Data at 150°F, Run 1.

T_sample	T_sink	pressure	I_sample_avg	I_lamp_avg	P/Po	Io/I	Io/I_lamp	ratioed
150.1004	72.90078	6.7	8.27101	5.503094	0.455782	0.806	1.000007	0.805994
149.9914	72.97461	7.7	7.900215	5.495332	0.52381	0.84383	1.00142	0.842633
149.9105	73.00625	8.7	7.578712	5.484429	0.591837	0.879627	1.003411	0.876637
149.9404	73.61621	9.7	7.397803	5.482355	0.659864	0.901137	1.00379	0.897735
150.1232	73.67598	10.7	7.148073	5.468584	0.727891	0.93262	1.006318	0.926765
150.0002	74.39141	11.7	7.102299	5.48451	0.795918	0.938631	1.003396	0.935454
150.0125	74.47227	12.7	6.928377	5.476294	0.863946	0.962193	1.004901	0.9575
149.951	74.50742	13.7	6.798933	5.499431	0.931973	0.980512	1.000674	0.979852
149.9773	74.50566	14.7	6.666437	5.503135	1	1	1	1
149.9404	74.51797	15.7	6.557498	5.519836	1.068027	1.016613	0.996974	1.019698
149.9281	74.83613	16.7	6.515841	5.538689	1.136054	1.023112	0.993581	1.029722
150.118	75.05234	17.7	6.432221	5.52301	1.204082	1.036413	0.996401	1.040156
150.0424	75.36348	18.7	6.357049	5.503611	1.272109	1.048669	0.999913	1.048759
149.8877	75.36348	19.7	6.2769	5.50535	1.340136	1.062059	0.999598	1.062487
150.023	75.64824	20.7	6.215552	5.516406	1.408163	1.072541	0.997594	1.075128
150.0617	75.85391	21.7	6.093198	5.447603	1.47619	1.094079	1.010194	1.083038
149.9527	75.83633	22.7	6.026583	5.443202	1.544218	1.106172	1.011011	1.094125

Table D10. Data at 150°F, Run 2.

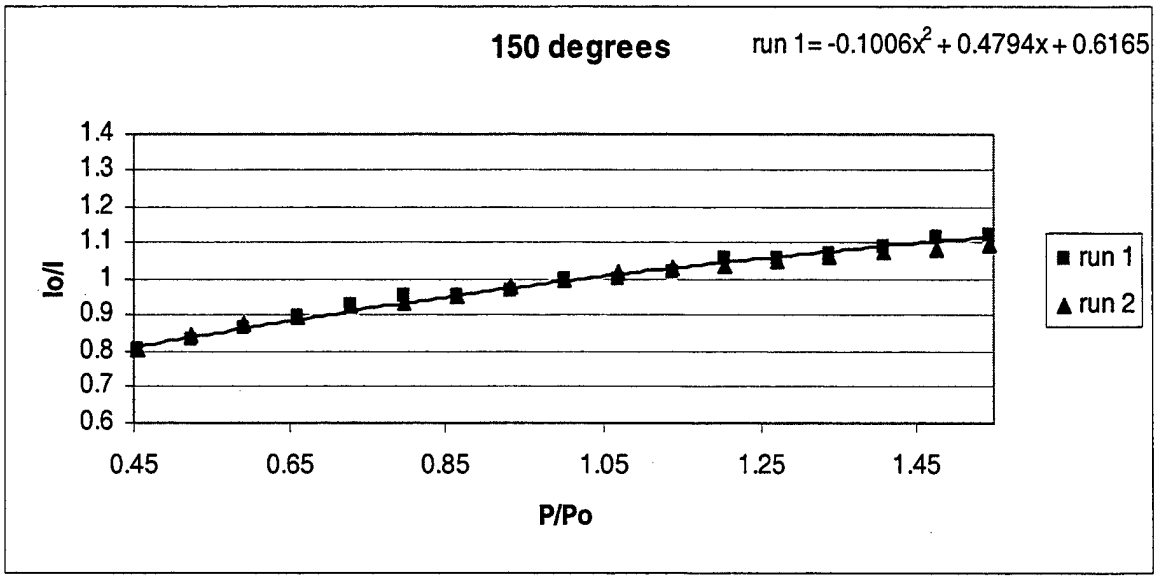

Figure D6. Plot of Io/I for Run 1 and Ratioed Data for Run 2 at 150°F.

(Note that in the above plot, run 1 is not ratioed due to inconsistent lamp data.)

T_sample	T_sink	pressure	I_sample_avg	I_lamp_avg	P/Po	Io/I	Io/I_lamp	ratioed
170.0129	74.15938	6.7	8.550396	8.188741	0.455782	0.768837	0.993321	0.774007
170.1096	74.71836	7.7	8.139421	8.214258	0.52381	0.807657	0.990235	0.815622
170.0006	75.67461	8.7	7.78488	8.157544	0.591837	0.84444	0.997119	0.846879
170.0867	76.04551	9.7	7.44386	8.074615	0.659864	0.883126	1.00736	0.876673
170.208	76.15801	10.7	7.189439	8.041425	0.727891	0.914378	1.011518	0.903966
170.1412	76.14746	11.7	7.003438	8.072211	0.795918	0.938662	1.00766	0.931527
170.0691	76.27578	12.7	6.787732	8.00127	0.863946	0.968492	1.016594	0.952683
170.0902	76.3584	13.7	6.627071	8.011127	0.931973	0.991971	1.015343	0.976981
170.0639	76.88926	14.7	6.573863	8.134045	1	1	1	1
170.0287	76.94375	15.7	6.462686	8.14281	1.068027	1.017203	0.998924	1.018299
169.9795	77.1125	16.7	6.387673	8.246558	1.136054	1.029148	0.986356	1.043384
170.0639	77.18281	17.7	6.236507	8.150092	1.204082	1.054094	0.998031	1.056173
170.1641	77.20039	18.7	6.160619	8.18147	1.272109	1.067078	0.994203	1.0733
170.0217	77.2584	19.7	6.067845	8.158282	1.340136	1.083393	0.997029	1.086622
169.9883	77.34453	20.7	5.986827	8.169702	1.408163	1.098055	0.995635	1.102868
169.9373	77.45703	21.7	5.932678	8.200403	1.47619	1.108077	0.991908	1.117116
170.1447	77.52207	22.7	5.823513	8.09776	1.544218	1.128848	1.004481	1.123813

Table D11. Data at 170°F, Run 1.

T_sample	T_sink	pressure	I_sample_avg	I_lamp_avg	P/Po	Io/I	Io/I_lamp	ratioed
170.034	75.52344	6.7	7.345519	9.9E+36	0.455782	0.862603	10	0.08626
170.041	77.07207	7.7	7.042514	7.92E+37	0.52381	0.899717	1.25	0.719773
170.0445	77.93516	8.7	6.818625	8.91E+37	0.591837	0.929259	1.111111	0.836333
170.0305	78.50469	9.7	6.687936	9.9E+37	0.659864	0.947418	1	0.947418
170.048	78.84922	10.7	6.479931	9.9E+37	0.727891	0.97783	1	0.97783
170.1641	79.09883	11.7	6.451298	9.9E+37	0.795918	0.98217	1	0.98217
170.0498	79.35898	12.7	6.593837	9.9E+37	0.863946	0.960938	1	0.960938
170.0182	79.48027	13.7	6.452384	9.9E+37	0.931973	0.982004	1	0.982004
170.0076	79.62969	14.7	6.336268	9.9E+37	1	1	1	1
170.0252	79.70176	15.7	6.29415	9.9E+37	1.068027	1.006692	1	1.006692
170.0867	79.81953	16.7	6.188271	9.9E+37	1.136054	1.023916	1	1.023916
170.0779	79.86875	17.7	6.081444	9.9E+37	1.204082	1.041902	1	1.041902
170.1025	79.81074	18.7	5.953605	9.9E+37	1.272109	1.064274	1	1.064274
169.9514	79.83184	19.7	5.893369	4.95E+37	1.340136	1.075152	2	0.537576
170.0867	79.82656	20.7	5.818449	9.9E+37	1.408163	1.088996	1	1.088996
170.1166	79.83008	21.7	5.765458	9.9E+37	1.47619	1.099005	1	1.099005
170.0762	79.87051	22.7	5.726616	9.9E+37	1.544218	1.106459	1	1.106459

Table D12. Data at 170°F, Run 2.

T_sample	T_sink	pressure	I_sample_avg	I_lamp_avg	P/Po	Io/I	Io/I_lamp	ratioed
170.1008	74.47227	6.7	7.521893	8.902817	0.455782	0.826439	0.997056	0.828879
170.041	75.75371	7.7	7.362946	8.840603	0.52381	0.844279	1.004072	0.840855
170.1148	75.91367	8.7	7.07562	8.854468	0.591837	0.878564	1.0025	0.876373
170.0217	75.93652	9.7	6.829258	8.860437	0.659864	0.910257	1.001825	0.908599
170.099	76.40938	10.7	6.693223	8.876331	0.727891	0.928758	1.000031	0.928729
170.0867	76.81895	11.7	6.605335	8.945947	0.795918	0.941115	0.992249	0.948467
170.1078	77.12656	12.7	6.48901	8.957629	0.863946	0.957986	0.990955	0.966731
170.0621	77.4043	13.7	6.400336	9.038531	0.931973	0.971259	0.982085	0.988976
170.0393	77.57832	14.7	6.216383	8.876605	1	1	1	1
170.0445	77.77871	15.7	6.118745	8.921527	1.068027	1.015957	0.994965	1.021099
170.1008	77.94922	16.7	6.014833	8.948627	1.136054	1.033509	0.991952	1.041894
170.0076	78.01602	17.7	5.908781	8.919232	1.204082	1.052058	0.995221	1.057111
169.9988	78.16543	18.7	5.826832	8.935858	1.272109	1.066855	0.993369	1.073976
170.0797	78.22871	19.7	5.739158	8.943726	1.340136	1.083152	0.992495	1.091343
169.9971	78.32363	20.7	5.62444	8.850049	1.408163	1.105245	1.003001	1.101938
170.0129	78.38691	21.7	5.541147	8.855621	1.47619	1.121859	1.00237	1.119207
170.0059	78.4748	22.7	5.470486	8.875165	1.544218	1.136349	1.000162	1.136165

Table D13. Data at 170°F, Run 3.

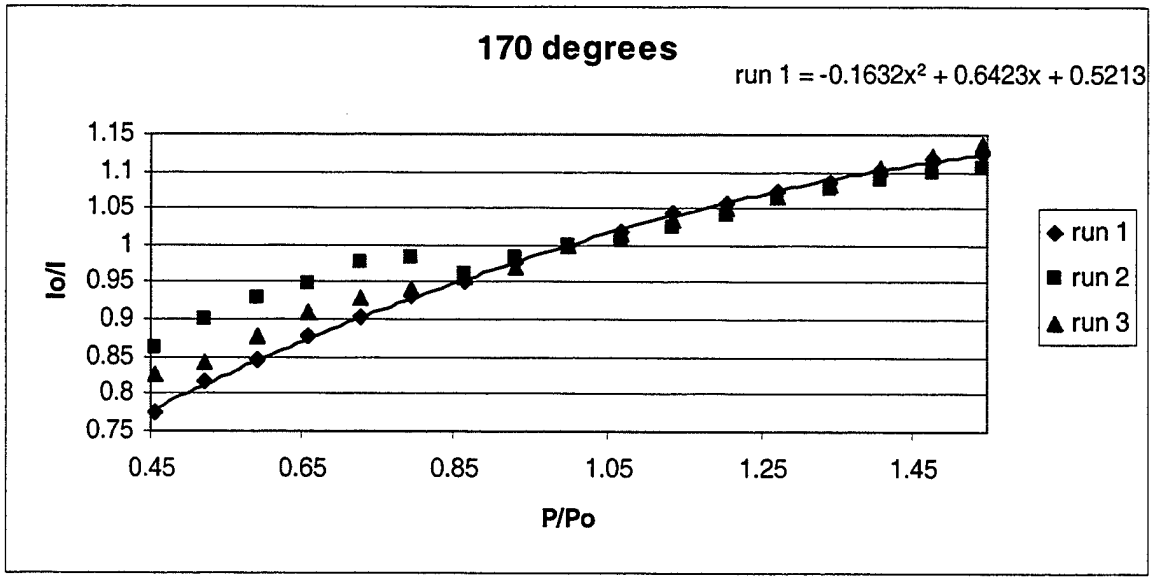

Figure D7. Plot of Ratioed Data for Run 1 and Io/I for Runs 2 and 3 at 170°F.

(Note that in the above plot, runs 2 and 3 are not ratioed due to inconsistent lamp data.)

The following plot was taken at constant pressure, varying temperature.

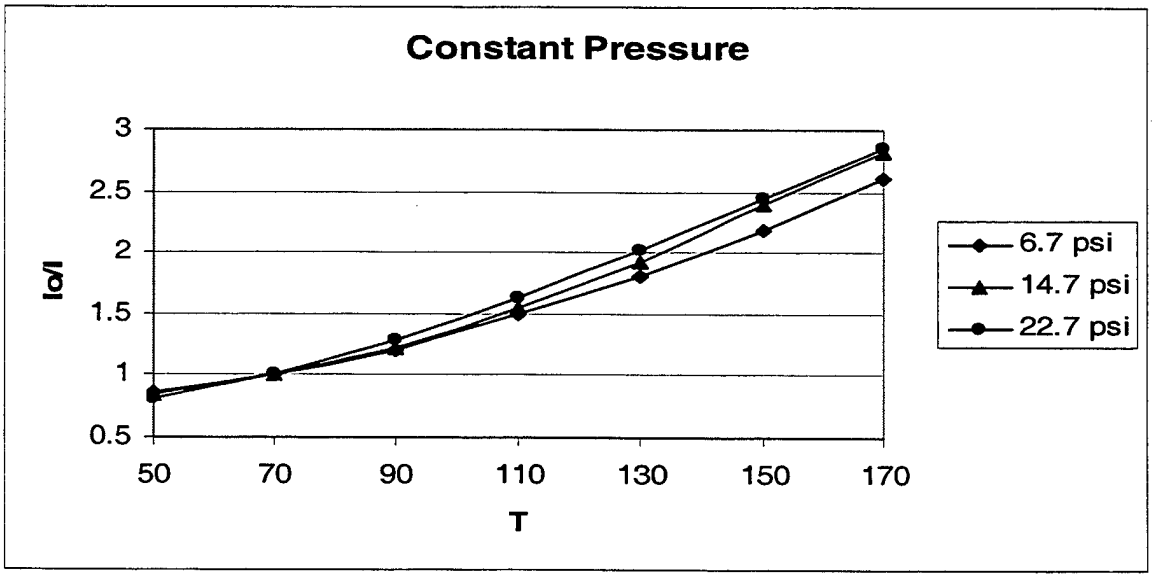

Figure D8. Constant Pressure Curves.

THIS PAGE INTENTIONALLY LEFT BLANK

APPENDIX E. CALIBRATION DATA

The following is a complete set of data curves, and the calibration functions based on the complete set of data. In cases where more than one run was made at a particular temperature, the best curve was used. As is evident from Figure E1, several curves do not follow the expected pattern. In particular, the 70° and 150° runs seem to be erroneous; therefore, they were left out of the calibration presented in the main body of the present work. The calibration curves for the complete data set are shown here. The F_I calibration curve, Figure E4, is also included although it was not used for this calibration. If the paint was used to determine the pressure mapping on a model, the F_I calibration curve would be necessary.

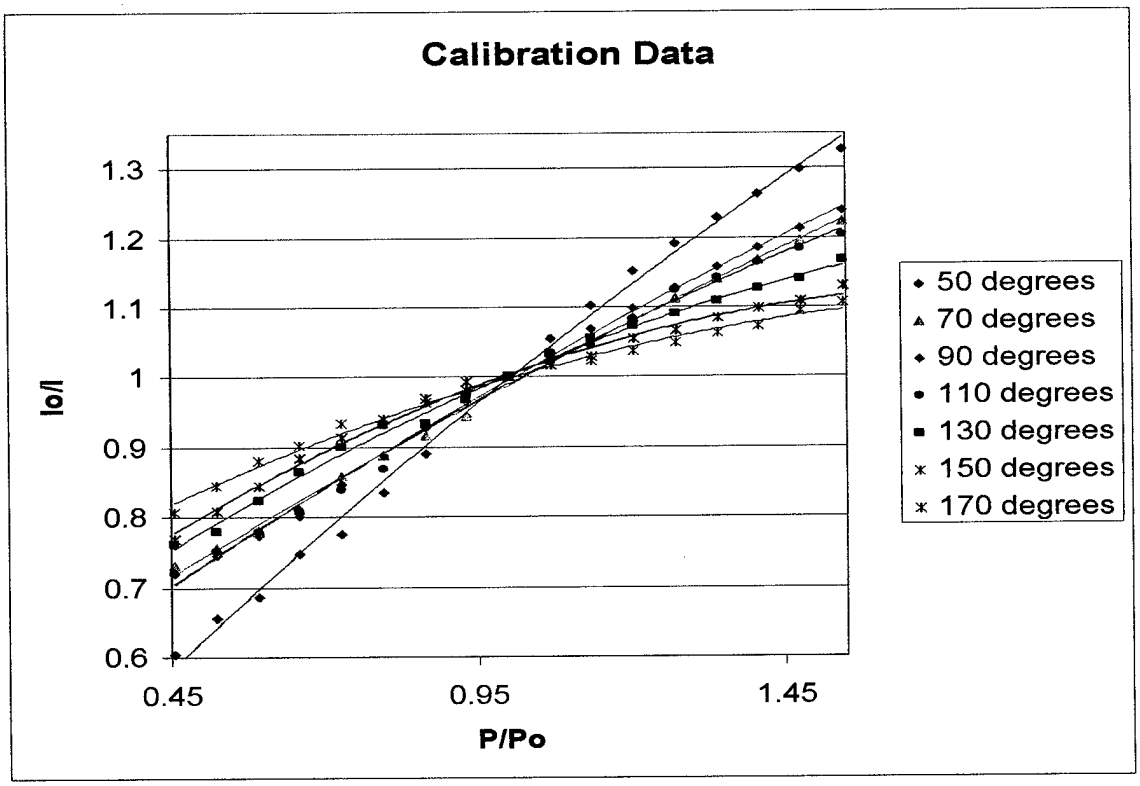

Figure E1. Complete Set of Calibration Curves.

T	A	B	C	T/Tref	A/Aref	B/Bref	Io at Po	Io/Ioref	A+B+C
50	0.1958	0.9065	-0.1055	0.555556	0.462556	1.399352	9.195375	0.560992	0.9968
70	0.4697	0.572	-0.0524	0.777778	1.109615	0.882989	12.307	0.750825	0.9893
90	0.4233	0.6478	-0.0755	1	1	1	16.39129	1	0.9956
110	0.4695	0.6026	-0.0778	1.222222	1.109142	0.930225	13.42835	0.819237	0.9943
130	0.4828	0.6667	-0.1477	1.444444	1.140562	1.029176	9.64632	0.588503	1.0018
150	0.6165	0.4794	-0.1006	1.666667	1.456414	0.740043	6.903845	0.42119	0.9953
170	0.5211	0.643	-0.1635	1.888889	1.231042	0.99259	6.573863	0.401058	1.0006

Table E1. Complete Set of Calibration Coefficients.

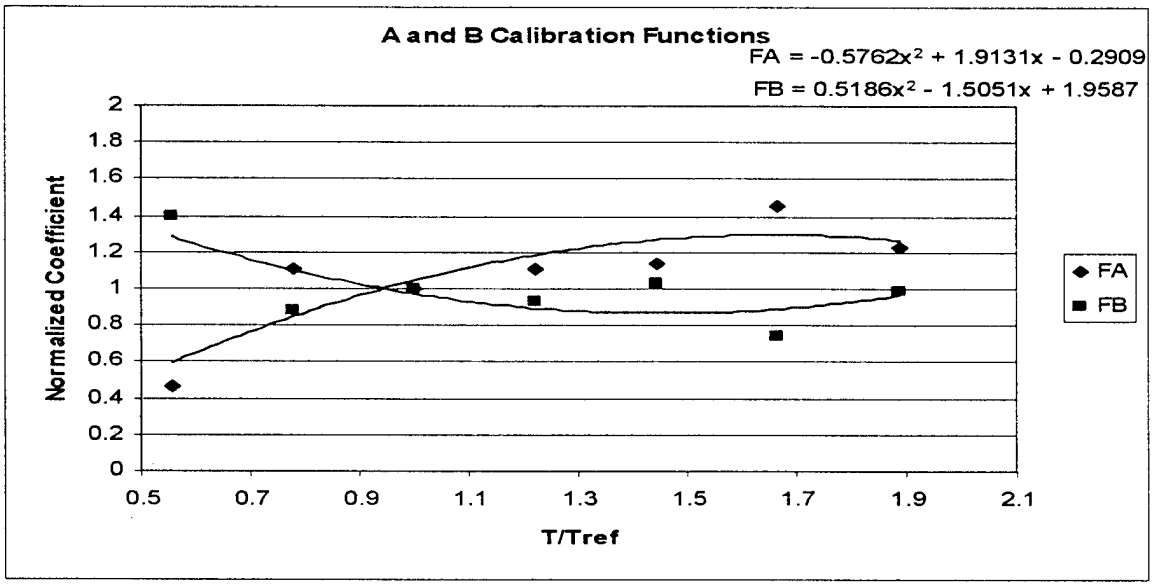

Figure E2. F_A and F_B Using All Data Points.

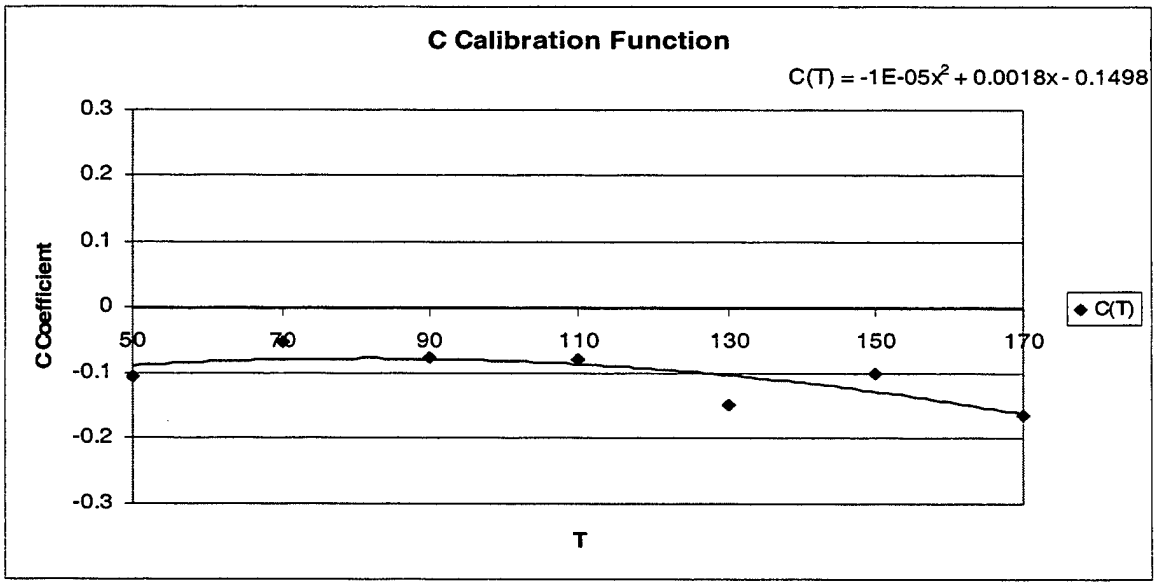

Figure E3. F_C Using All Data Points.

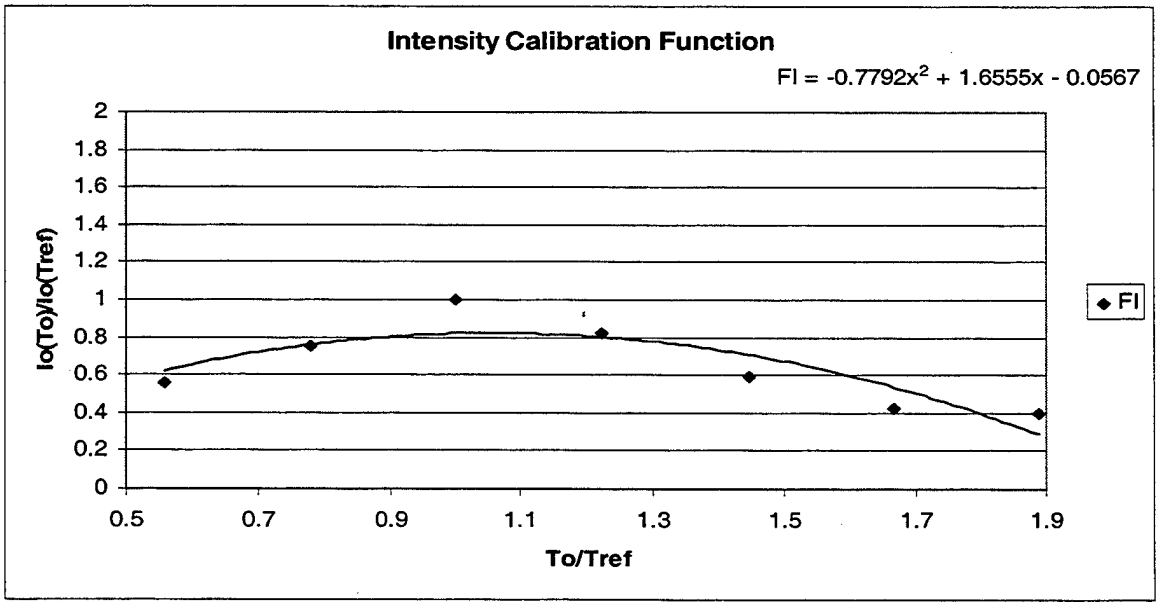

Figure E4. F_I Using All Data Points.

THIS PAGE INTENTIONALLY LEFT BLANK

LIST OF REFERENCES

(1) Grossman, B.L., "Testing and Analysis of a Transonic Axial Compressor", Master's Thesis, Naval Postgraduate School, Monterey, Ca, September 1997.

(2) Varner, D.R., "Pressure Sensitive Paint Measurement on a Rotor", Master's Thesis, Naval Postgraduate School, Monterey, Ca, March 1995.

(3) Quinn, K.J., "Pressure Sensitive Paint Measurement Technique Development for Turbomachinery Application", Engineer's Thesis, Naval Postgraduate School, Monterey, Ca, December 1997.

(4) Baumann, P.D., "Investigation of Pressure and Temperature Sensitivities of a Pressure Sensitive Paint", Master's Thesis, Naval Postgraduate School, Monterey, Ca, September 1998.

(5) Seivwright, D.L., "Application of Pressure-Sensitive Paint in Shock-Boundary Layer Interaction Experiments", Master's Thesis, Naval Postgraduate School, Monterey, Ca, March 1996.

(6) Kavandi, J.L., "Luminescence Imaging for Aerodynamic Pressure Measurements", Doctoral Thesis, Chemistry Department, University of Washington, 1990.

(7) Bell, J.H., Private Conversations, NASA-Ames Research Center, Moffett Field, Ca., January - March 2000.

(8) Woodmansee, M.A., and Dutton, J.C., "Methods for Treating Temperature Sensitive Effects of Pressure-Sensitive Paints", AIAA Paper No. 97-0387, Presented at the 35th Aerospace Sciences Meeting and Exhibition, Reno, Nevada, January 6-10, 1997.

(9) Shreeve, R.P., *Unpublished Notes*, Naval Postgraduate School, Monterey, Ca, September 1998.

THIS PAGE INTENTIONALLY LEFT BLANK

INITIAL DISTRIBUTION LIST

1. Defense Technical Information Center 2
   8725 John J. Kingman Road, Suite 0944
   Ft. Belvoir, VA 22060-6218

2. Dudley Knox Library 2
   Naval Postgraduate School
   411 Dyer Road
   Monterey, CA 93943-5101

3. Chairman, Code AA 1
   Department of Aeronautics and Astronautics
   Naval Postgraduate School
   699 Dyer Road, Room 137
   Monterey, California 93943-5106

4. Professor R. P. Shreeve, Code AA/SF 5
   Department of Aeronautics and Astronautics
   Naval Postgraduate School
   699 Dyer Road, Room 137
   Monterey, California 93943-5106

5. Assoc. Professor G. V. Hobson, Code AA/HG 1
   Department of Aeronautics and Astronautics
   Naval Postgraduate School
   699 Dyer Road, Room 137
   Monterey, California 93943-5106

6. Naval Air Warfare Center – Aircraft Division 1
   Propulsion and Power Engineering
   ATTN: J. Zidzik, Code 4.4.7.1, BLDG 106
   22195 Elmer RD, Unit 4
   Patuxent River, Maryland 20670-1534

7. Naval Air Warfare Center – Aircraft Division 1
   Propulsion and Power Engineering
   ATTN: M. Klein, Code 4.4.7.1, BLDG 106
   22195 Elmer RD, Unit 4
   Patuxent River, Maryland 20670-1534

8. Naval Air Warfare Center – Aircraft Division 1
Propulsion and Power Engineering
ATTN: C. Gorton, Code 4.4.T, BLDG 106
22195 Elmer RD, Unit 4
Patuxent River, Maryland 20670-1534

9. ENS Judith A. Muller 1
318 Gilbert St.
Ridgewood, NJ 07450